Neuroscience and Biobehavioral Reviews 123 (2021) 83–103

Contents lists available at ScienceDirect

Neuroscience and Biobehavioral Reviews

journal homepage: www.elsevier.com/locate/neubiorev

Review article

Updating and characterizing neuroanatomical markers in high-risk subjects, recently diagnosed and chronic patients with schizophrenia: A revised coordinate-based meta-analysis

Donato Liloia [a,b], Claudio Brasso [c], Franco Cauda [a,b,d,*], Lorenzo Mancuso [a,b], Andrea Nani [a,b], Jordi Manuello [a,b], Tommaso Costa [a,b,d], Sergio Duca [a,b], Paola Rocca [c,d]

[a] GCS-fMRI, Koelliker Hospital and Department of Psychology, University of Turin, Turin, Italy
[b] Functional Neuroimaging and Complex Neural Systems (FOCUS) Laboratory, Department of Psychology, University of Turin, Turin, Italy
[c] Department of Neuroscience "Rita Levi Montalcini", University of Turin, Turin, Italy
[d] Neuroscience Institute of Turin (NIT), University of Turin, Turin, Italy

ARTICLE INFO

Keywords:
Schizophrenia
Ultra-high risk
Activation likelihood estimation
Psychosis
Voxel-based morphometry
Signed differential mapping
Behavioral analysis
Coordinate-based meta-analysis
Salience network

ABSTRACT

Characterizing neuroanatomical markers of different stages of schizophrenia (SZ) to assess pathophysiological models of how the disorder develops is an important target for the clinical practice. We performed a meta-analysis of voxel-based morphometry studies of genetic and clinical high-risk subjects (g-/c-HR), recently diagnosed (RDSZ) and chronic SZ patients (ChSZ). We quantified gray matter (GM) changes associated with these four conditions and compared them with contrast and conjunctional data. We performed the behavioral analysis and networks decomposition of alterations to obtain their functional characterization. Results reveal a cortical-subcortical, left-to-right homotopic progression of GM loss. The right anterior cingulate is the only altered region found altered among c-HR, RDSZ and ChSZ. Contrast analyses show left-lateralized insular, amygdalar and parahippocampal GM reduction in RDSZ, which appears bilateral in ChSZ. Functional decomposition shows involvement of the salience network, with an enlargement of the sensorimotor network in RDSZ and the thalamus-basal nuclei network in ChSZ. These findings support the current neuroprogressive models of SZ and integrate this deterioration with the clinical evolution of the disease.

1. Introduction

Schizophrenia (SZ) is a severe psychiatric disorder with a typical onset in late adolescence or early adulthood (Owen et al., 2016). The disability-associated burden of SZ was 13.4 million years lived with disability (YLDs) worldwide, equivalent to 1.7 % of global YLDs in 2016 (Charlson et al., 2018).

Considered the heavy burden of SZ, a better comprehension of the pathophysiology of this disorder is needed to improve treatments and outcomes (Wojtalik et al., 2017). Various current pathophysiological paradigms consider SZ as a neurodevelopmental disease with a progressive peculiar neurodegenerative component characterized by reduced dendritic spines density, altered synaptic homeostasis and glial dysfunction in the absence of gliosis and neuronal necrosis (Andreasen, 2010; Ashe et al., 2001; Buoli et al., 2017; Velakoulis et al., 2000). According to this hypothesis, specific abnormalities, taking place in precise brain development stages, are associated with SZ onset and followed by processes of brain aging acceleration (Buoli et al., 2017; Nenadic et al., 2017). This type of brain alteration can manifest as a progressive reduction in the gray matter (GM) volume of specific neural territories. SZ could be staged from an increased risk of developing psychosis, with milder observable neurobiological and clinical expressions, to a persistent and unremitting condition with more evident signs of neurodegeneration (Davis et al., 2014; McGorry et al., 2006; Ortiz et al., 2017; Wood et al., 2011).

In-vivo neuroimaging techniques have provided an unprecedented insight into the brain alterations underlying neuropsychiatric disorders. Among them, one of the most employed approaches is the structural

* Corresponding author at: Department of Psychology, University of Turin, via Giuseppe Verdi 10, 10124, Torino, Italy.
E-mail addresses: donato.liloia@unito.it (D. Liloia), claudio.brasso@unito.it (C. Brasso), franco.cauda@unito.it (F. Cauda), lorenzo.mancuso@unito.it (L. Mancuso), andrea.nani@unito.it (A. Nani), jordi.manuello@unito.it (J. Manuello), tommaso.costa@unito.it (T. Costa), ducasergio@osp-koelliker.it (S. Duca), paola.rocca@unito.it (P. Rocca).

https://doi.org/10.1016/j.neubiorev.2021.01.010
Received 15 June 2020; Received in revised form 7 January 2021; Accepted 15 January 2021
Available online 23 January 2021

magnetic resonance imaging (sMRI) with voxel-based morphometry (VBM) (Isobe et al., 2016). VBM allows the detection of GM focal variations (i.e. volume or concentration) between-subject groups comparisons by means of a quantitative and voxel-wise analysis (for a detailed explanation of the method see Ashburner and Friston, 2000). Starting from the seminal work of Wright et al. (1995), widespread morphometric reductions have been repeatedly reported in groups of patients with SZ compared to healthy controls (HC). Importantly, some abnormalities have been observed both at first presentation and in the chronic stage of illness. In this regard, the systematic review of Shepherd et al. (2012) suggested that multiple GM degenerations occur regardless of SZ stages, encompassing the insulae, frontal gyri (particularly the inferior and medial ones), right anterior cingulate and superior temporal cortices. However, the conclusive picture of shared brain markers was limited by the heterogeneity quality of voxel-based investigations being reviewed (Shepherd et al., 2012). Moreover, some authors detected volumetric loss only in isolated cerebral loci (Ferri et al., 2012; Nakamura et al., 2013; Zhang et al., 2015) or even clusters of GM increase (Oertel-Knöchel et al., 2012; Sheng et al., 2013; Watson et al., 2012).

Despite substantial advances in sMRI research on SZ, replicability of results is still far from satisfactory (Hager and Keshavan, 2015; John et al., 2015; Kochunov et al., 2019). Potential sources of variability in findings may be partially due to differences in the assessed clinical population in terms of duration of illness (recently diagnosed or chronic SZ vs. mixed) (Torres et al., 2016), diagnoses included (only SZ vs. SZ spectrum disorders) (Fervaha and Remington, 2013; Rink et al., 2016; Velakoulis et al., 2006), medical comorbidities or substance abuse (Bora et al., 2017; Koenders et al., 2015), gender distribution (Bora et al., 2012), medication status (antipsychotic-naïve vs. -treated) (Torres et al., 2013), age and type of symptomatology (Koutsouleris et al., 2014). Other confounding factors could derive from methodological choices regarding the type of analysis (whole-brain vs. region of interest - ROI or small volume correction -SVC) (McDonald et al., 2008; Voormolen et al., 2010), acquisition protocols (Jovicich et al., 2009), preprocessing software packages (Li et al., 2019a), sample size (small vs. multicenter mega-analyses) (Torres et al., 2016) and statistical thresholding procedures (Bennett et al., 2009; Vijayakumari et al., 2015).

Given these many confounding factors in the between-group comparisons, an objective assessment is needed to provide robust findings and summarize the recent growing literature about neuroanatomical alterations in SZ. A powerful approach is the quantitative synthesis of published neuroimaging results by means of coordinate-based meta-analysis (CBMA). In particular, the anatomical likelihood estimation (ALE) represents the most widely employed technique in the CBMA field (Tahmasian et al., 2019) and is able to quantify convergent morphometric alterations of neuropsychiatric disorders in a fully automated and replicable manner (Eickhoff et al., 2012). The ALE provides a rigorous environment to estimate the probability of spatial-unbiased distribution maps across experiments, mitigating the laboratory and group-level inhomogeneity (Fox et al., 2014).

This technique and other CBMA approaches have been usefully employed in the last two decades, suggesting that distributed cortical, subcortical and cerebellar GM alterations are involved in SZ spectrum disorders (Bora et al., 2011; Chan et al., 2011; Ellison-Wright and Bullmore, 2010; Ellison-Wright et al., 2008; Fornito et al., 2009; Glahn et al., 2008; Li et al., 2018; Nickl-Jockschat et al., 2011). Also, the presence of aberrations in unaffected relatives of patients with SZ (genetic-risk) and in individuals at risk of psychosis (clinical-risk) has been convincingly highlighted (Fusar-Poli et al., 2011a, 2014; Saarinen et al., 2020). Although these meta-analytic findings are relevant, a considerable variability and inconsistency persist due to heterogeneity in the examined hypothesis and/or clinical sub-populations, different inclusion/exclusion criteria and, consequently, in the number of the analyzed experiments. In addition, certain important issues remain to be addressed.

Previous CBMAs systematically included several VBM experiments comparing HC with a mixed experimental group composed of individuals with SZ and of others with diagnoses belonging to the SZ spectrum disorders (SSD), so that the "pure" contribution of the diagnosis of SZ in GM alterations was not completely explored. For this reason, samples including patients diagnosed with SSD were not included in the present CBMA. The choice to focus on the SZ diagnosis only meets the need for identifying patterns of GM alterations that are specific to SZ. Furthermore, given that SZ is the most represented mental disorder in terms of number of sMRI studies and SZ diagnostic criteria are relatively stable over time and between nosological classifications, samples studied in different periods tend to be homogeneous.

We also decided to examine genetic and clinical high-risk (HR) states for psychosis because these two pre-psychotic conditions, albeit not necessarily evolving to psychosis, are characterized by GM alterations, which are not always consistent across studies (Cooper et al., 2014; Saarinen et al., 2020). From a clinical perspective, the detection of consensual neuroanatomical modifications can facilitate a prompt identification of these conditions by assessing their role in the transition to full-blown psychosis, as well as allow more effective strategies for prevention and care. Moreover, a number of studies on these HR samples are now available and sufficient to perform a robust CBMA.

Observer-independent functional characterization of the GM loss in different stages of SZ is essential in order to better understand how large-scale brain networks are involved in different periods of the disease progression. It is also of fundamental importance to control clinical, socio-demographic and methodological effects on VBM results in SZ (John et al., 2015; Kakeda and Korogi, 2010; Kambeitz et al., 2015; Vijayakumari et al., 2015). To our knowledge, no previous CBMAs on aberrant morphometric patterns linked to mental domains have been carried out so far. This line of research would provide a quantitative description of the functional and behavioral impact of anatomical variations at different stages of the disorder.

Another important aspect concerns the recent methodological innovations for the CBMA and the publication of best-practice protocols for this field. In 2017 the BrainMap team reported some technical errors affecting the ALE algorithm as implemented in GingerALE software, whose codes for the thresholding procedure may have increased the rate of false positives (Eickhoff et al., 2017). Still, different authors (Eickhoff et al., 2017, 2016; Müller et al., 2017; Samea et al., 2019) have strongly discouraged the use of the previously customary false discovery rate (FDR) voxel-level thresholding in the context of ALE meta-analyses, advising instead the use of cluster-level family-wise error (FWE) thresholding, given its better sensitivity to true effects. Great care was recommended regarding the inclusion of studies to enhance reliability and reproducibility, as well as to facilitate subsequent research efforts (Müller et al., 2018; Nichols et al., 2017; Tahmasian et al., 2019). In light of this, computational, statistical and reporting advances support the need to carry out a novel meta-analytic investigation. This is particularly true for an updated and extended estimation on different SZ stages, as the most recent ALE analysis on this topic dates back to 2011 (Chan et al., 2011) and many new relevant VBM studies were published since then.

We therefore conducted an exhaustive systematic search to revisit and characterize spatially consistent GM variations in four clinical groups: genetic high-risk subjects (g-HR), clinical high-risk subjects (c-HR), patients recently diagnosed with SZ (RDSZ, with a duration of illness - DOI < 2 years), and chronic SZ patients (ChSZ, DOI ≥ 2 years). The present ALE study is based on the largest data set of whole-brain VBM results included so far about this topic, on restrictive inclusion criteria, on stringent statistical procedure and on the most recent consensus-based protocols. Our aim has been to establish the most consistent neuroanatomical abnormalities related to the subsequent phases of the SZ. In order to derive common and potentially distinctive brain markers, contrast meta-analyses were conducted between the different groups. We also examined the effects of socio-demographic, clinical and methodological variables through voxel-wise meta-re-

gressions. Finally, we assessed the cognitive/behavioral profiles associated with the GM clusters of alteration identified by the ALE. This combination of morphometric localization and functional characterization allowed for observer-independent inference, thus linking statistically the SZ pathophysiology to its clinical manifestations.

2. Methods

2.1. Data identification

The study protocol adhered to the PRISMA Statement international guidelines (Moher et al., 2009) and current consensus recommendations for neuroimaging CBMA (Müller et al., 2018; Tahmasian et al., 2019). We employed the software application Sleuth (v.3.0.3) to query the VBM database of BrainMap (December 1, 2019) (Vanasse et al., 2018). We assembled a standardized search algorithm as follow:

- *"Experiments Context IS Disease Effects" AND "Subjects Diagnosis IS Schizophrenia" AND "Experiments Contrast IS Gray Matter" AND "Experiments Observed Changes IS Controls > Patients AND Controls < Patients".*

We also employed the PubMed search engine to perform a systematic literature search on the MEDLINE database. We used the Advanced Search Builder adopting the following terms to search in title/abstracts:

- *("voxel-based morphometry" OR "VBM" OR "voxel-wise") AND ("schizophrenia" OR "chronic schizophrenia" OR "SZ" OR "first episode schizophrenia" OR "first episode psychosis" OR "high risk schizophrenia" OR "siblings schizophrenia" OR "first degree relatives" OR "genetic risk schizophrenia" OR "at risk of mental state" OR "ARMS" OR "ultra-high risk").*

As final step, we screened references consulting previous review articles (Birur et al., 2017; Shepherd et al., 2012) and CBMAs about the conditions of interest (Chan et al., 2011; Ellison-Wright et al., 2008; Fusar-Poli et al., 2011a, 2014).

2.2. Data selection

The identified articles were systematically reviewed. Inclusion criteria for neuroimaging experiments were: (a) to be included in a research article published in a peer-review journal; (b) to use a specified whole-brain VBM analysis; (c) to report GM variations in HR subjects and/or patients with RDSZ and/or patients with ChSZ by means of a between-group comparison with healthy controls; (d) to report results in the form of stereotactic space (i.e. x,y,z coordinates in Talairach or MNI space); (e) to adopt analyses corrected for multiple comparisons or cluster-wise extent thresholds >100 voxels; (f) experimental group without other medical comorbidities; (g) diagnosis of SZ based on fulfilling ICD or DSM criteria.

Moreover, we applied rigorous and restrictive exclusion criteria according to which we excluded the articles with one or more of the following characteristics: (a) experimental groups with a sample size < 10 subjects; (b) use of ROI or SVC analysis; (c) mixed experimental sample (i.e. SZ and other SDDs and/or RDSZ and ChSZ). Still, to avoid the possibility of analyzing the same subjects several times in a single study, we selected only the alteration foci reported by the analysis with the largest sample of that study. Furthermore, to prevent redundancy of subjects and related results across studies by the same authors we selected only the last study (more recent publication date) published by the same research group with the same sample. Detailed reporting of inclusion and exclusion criteria can be found in the best-practice checklist (**Table S1**).

2.3. Clinical groups definition

Following the seminal ALE study of Chan et al. (2011), we partitioned our data set into distinct clinical groups: HR, RDSZ and ChSZ. However, we divided HR subjects into two groups (genetic and clinical HR) according to the model proposed by Fusar Poli et al. (2011a). The HR sample consisted of subjects at risk of developing SZ and was composed by the genetic HR group (g-HR) represented by monozygotic twins, siblings and first/second-degree relatives of patients with SZ and the clinical HR group (c-HR) of individuals at risk mental state (ARMS) meeting the criteria of either the Personal Assessment and Crisis Evaluation (PACE) (Yung et al., 1998), the Comprehensive Assessment of At-Risk Mental States (CAARMS) (Yung et al., 2005) or the Structured Interview for Prodromal Symptoms (SIPS) (Miller et al., 2003). The RDSZ group was composed of subjects with DOI less than 2 years. In the ChSZ group, patients had DOI equal or greater than 2 years. We included investigations that, though not reporting the DOI, referred clearly to a whole RDSZ or ChSZ sample.

2.4. Anatomical likelihood estimation

A series of ALE meta-analyses was conducted to determine a consistent pattern of GM variations for each of the four clinical groups and for all schizophrenia patients. A revised version of the ALE algorithm implemented in GingerAle (v.3.0.2) was applied (Turkeltaub et al., 2012). Following the recently recommended ALE setting (Eickhoff et al., 2017, 2016), ALE results were family-wise error-corrected (FWE-c) for multiple comparisons, with a cluster-level inference of $p < .05$ and a cluster-forming threshold of $p < .001$ on the voxel-level. We conducted analyses in Talairach space. Thus, we used the icbm2tal algorithm to convert the MNI coordinates into TAL space, improving the accuracy of meta-analysis (Lancaster et al., 2007).

The ALE technique provides information about the spatial convergence of results of the existing literature, considering every coordinate reported in a given study as being the center of a Gaussian probability distribution calculated as:

$$(d) = \frac{1}{\sigma^3\sqrt{(2\pi)^3}} e^{\frac{d^2}{2\sigma^2}}$$

in which d is the Euclidean distance between the coordinate and the surrounding voxels, and σ represents the spatial uncertainty. For each experiment we calculated a modeled alteration (MA) map, considered as the union of every Gaussian distribution of probability related to a given experiment. The combination of all the MA maps resulted in the final ALE map. The significance of each voxel was then tested against a null hypothesis obtained by an iterative random distribution of the foci, and the cluster-level threshold was determined with a Monte Carlo simulation of a cluster size distribution (10,000 permutations).

Finally, contrast analyses were performed (Eickhoff et al., 2011) in order to identify statistically significant differences and convergence between the clinical groups using a $p < .01$ and minimum cluster-size of 10 mm^3 (10,000 permutations).

2.5. Standard voxel-wise permutation tests

We further interrogated the presence of GM variations in our clinical groups by using voxel-wise permutation tests as implemented in the FSL's randomise algorithm (https://fsl.fmrib.ox.ac.uk/fsl/fslwiki/Randomise; Winkler et al., 2014). Starting from the unthresholded MA maps, this algorithm was able to conduct a standard permutation of subject-based images (PSI) to test the presence/absence of the effect in a given voxel, rather than testing the convergence of independent findings around the voxel as implemented in the current CBMA methods (Albajes-Eizagirre and Radua, 2018; Albajes-Eizagirre et al., 2019). For each clinical group, results of test statistics were family-wise error-corrected

(FWE-c) for multiple comparisons on the cluster-level with 5,000 permutation runs. Maps were thresholded at $p < .05$, corresponding to a z-score value ≥ 2.3.

2.6. Behavioral characterization

Analysis of behavioral domain profiles aims to statistically link morphometric clusters with corresponding physiological mental processes by testing which functional neuroimaging task is more likely to activate a given cluster. The rationale behind this approach is to provide a quantitative and data-driven attribution of psychological processes to neural subpopulations, respect to a qualitative interpretation of structural results.

We functionally characterized areas of alteration derived by our ALE meta-analyses using the Behavioral plugin (v.3.1) implemented in the Mango software package (Lancaster et al., 2012), capable of testing activation foci of the BrainMap database. At the time of analysis, BrainMap contained over 9400 functional experiments in healthy subjects, each of which has been classified according to the specific mental operations isolated by its experimental contrast into five behavioral domains: (1) cognition, which comprises neuro- and social cognition, with special attention to two cognitive processes: memory and language; (2) perception, referred to external stimuli such as auditory and visual stimuli; (3) interoception, referred to internal stimuli such as hunger, heartbeat and sexual libido; (4) emotion, comprising positive and negative emotions; and (5) action, defined as mental faculty associated with overt movements of the body. Mental operations are further divided into 51 subdomains (see full taxonomy list at http://brainmap.org/taxonomy/behaviors.html) belonging to the five aforementioned domains.

Behavioral analyses were performed separately on each clinical group both on the entire pattern of alteration at a whole-brain level and on each derived ALE cluster. A threshold of $p < .05$ with Bonferroni correction for multiple comparisons was applied, corresponding to a subdomain z-score ≥ 3.

2.7. Network decomposition

We investigated the impact of GM alterations on functional large-scale networks, detecting how many altered volumes (mm^3) derived from the ALE map of each clinical group fell within different networks. The rationale behind this approach is to provide a quantitative description of the functional localization of anatomical variations, as well as to evaluate a possible evolution and enlargement of the pattern at different stages of the disorder. We applied the 20-network parcellation proposed by Biswal et al. (2010), which parceled human brain cortex using resting-state functional MRI data from 1414 healthy subjects. Decomposition analyses were carried out separately for each clinical group, calculating the number of altered volumes belonging to each of the 20 functional networks and the percentage of alterations of each network, defined as the ratio between the number of altered voxels belonging to a given network and the total number of altered voxel of the ALE map of GM decrease of that clinical group.

2.8. Meta-regression

Using the Signed Differential Mapping software (i.e. anisotropic kernel effect sizes version, AES-SDM, v.6.12) (Radua et al., 2014), a series of voxel-wise meta-regression analyses were conducted to explore the potential effects of gender, positive and negative symptoms, age and antipsychotic treatment in the whole SZ sample. Effects of sample size, MRI field strength, slice thickness and image smoothing level were also examined. VBM experiments that did not report these measures were excluded from analyses. A voxel-level threshold of $p < .0005$ with a minimum cluster size of 10 voxels was adopted as proposed by Radua et al. (2012), to offer an optimal balance of specificity and sensitivity in terms of results.

AES-SDM is a relatively new CBMA method that borrows several characteristics from ALE, particularly the kernel-based rationale and the implementation of the coordinate-based random-effects approach; it is therefore able to combine the information of alteration foci in stereotactic space across independent experiments (for a detailed explanation of the methods see also Radua and Mataix-Cols, 2012; Samartsidis et al., 2017). The novelty of SDM consists in incorporating t-value statistics related to alteration foci (i.e. effect size estimation), and in the possibility of addressing the confounding effect of potential moderators across included experiments. Meta-regression investigation was conducted via AES-SDM, as we thought it could complement our main analyses for two reasons: (a) meta-regression is to date a largely unexplored topic in CBMA research, particularly valuable when meta-analyzed experiments exhibit an appreciable heterogeneity (Samartsidis et al., 2017), as it is the case of SZ; (b) the comparison between the ALE and SDM yielded similar results in term of spatial convergence for both simulated and empirical data sets (Albrecht et al., 2019; Eickhoff et al., 2016; Enge et al., 2020; Radua and Mataix-Cols, 2012; Samartsidis et al., 2017; Vitolo et al., 2017). We thus expect that ALE map related to the whole SZ group is indicative of AES-SDM method as well.

3. Results

Based on the search strategy, 113 peer-reviewed VBM articles were included, for a total of 124 between-group experiments, 11,270 subjects (5,263 in the four clinical groups and 6,007 HC) and 1,104 coordinates of GM variation (1,042 of decrease and 62 of increase) (Fig. 1).

In details, the g-HR group (average age = 28.7 years) included 18 experiments, 927 subjects compared with 910 HC and 76 coordinates of alteration (64 of GM decrease and 12 of GM increase). The c-HR group (average age = 22.4 years) included 16 experiments, 580 subjects compared with 621 HC and 67 coordinates of alteration (59 of GM decrease and 8 of GM increase). The RDSZ group (average age = 22.8 years; mean illness duration = 0.8 years) included 41 experiments, 1,636 subjects, 1,953 HC and 388 coordinates of alteration (359 of GM decrease and 29 of GM increase). The ChSZ group (average age = 38.6 years; mean illness duration = 15.0 years) included 49 experiments, 2,120 subjects, 2,563 HC and 573 coordinates of alteration (560 of GM decrease and 13 of GM increase). The best-practice checklist for CBMA (Müller et al., 2018) was reported in **Table S1**. Detailed information about the sample of each included experiment is summarized in **Tables S2** and **S3**. Distribution of the included experiments in the four clinical groups is summarized in **Table S4**.

ALE analysis was performed only for GM reduction foci, as the number of VBM experiments reporting GM increases (i.e. g-HR = 6 experiments; c-HR = 4; RDSZ = 7; ChSZ = 7; **Table S3**) was insufficient to achieve robust ALE estimates (Eickhoff et al., 2016).

3.1. ALE meta-analyses on different stages of schizophrenia

GM reductions in g-HR, c-HR, RDSZ and ChSZ groups relative to HC are shown in Table 1 and Figs. 2–4. Results of the ALE meta-analysis performed on the whole sample of patients diagnosed with schizophrenia (RDSZ and ChSZ groups pooled together) are shown in **Table S5** and **Fig. S1**.

3.1.1. g-HR vs. controls

The g-HR group showed no significant cluster of variation.

3.1.2. c-HR vs. controls

The c-HR group showed a single cluster of GM reduction (altered volume = 800 mm^3), with the ALE maximum value located in the right anterior cingulate cortex (R-ACC, Brodmann area -BA 32).

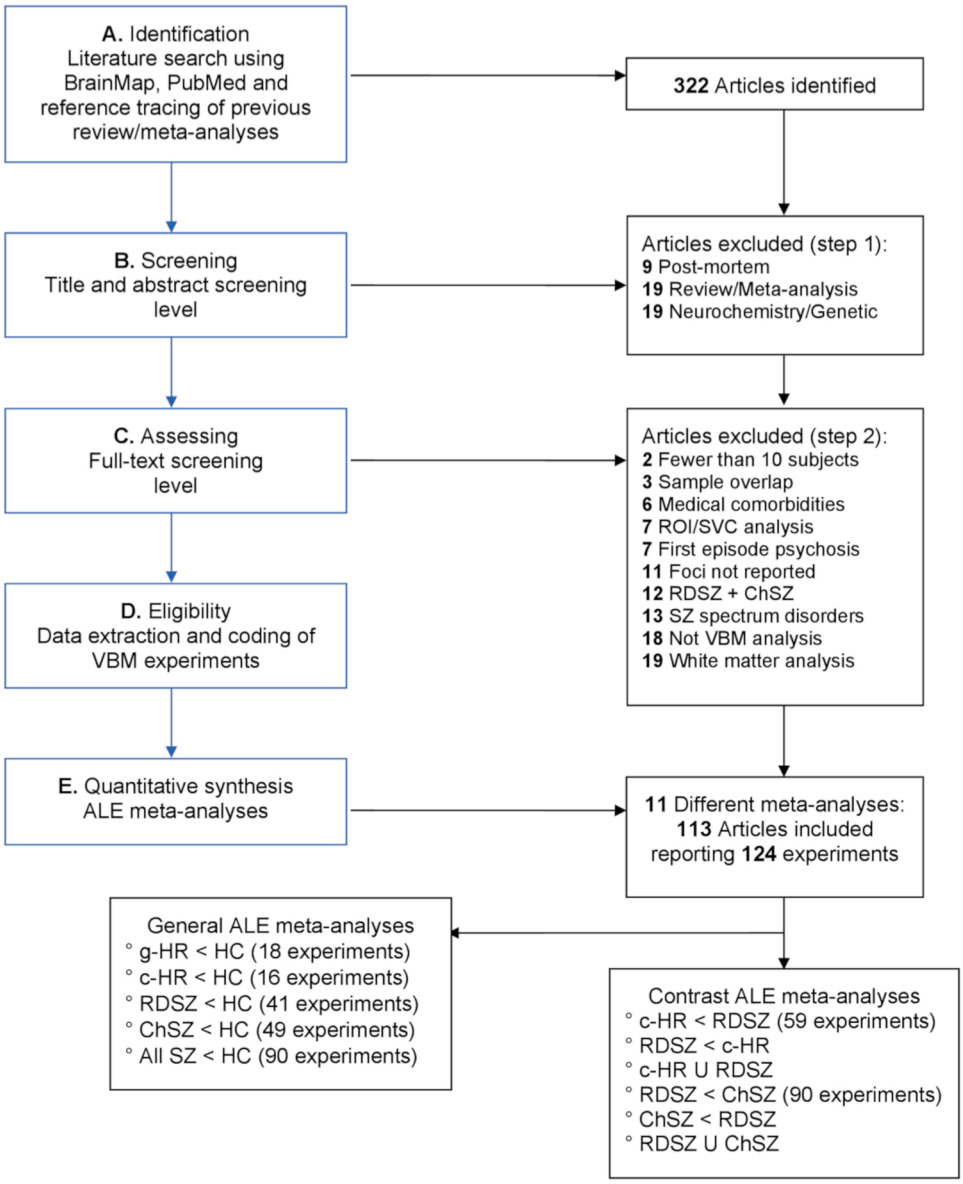

Fig. 1. Study selection overview and meta-data organization - PRISMA flow chart.
g-HR: genetic high-risk; c-HR: clinical high-risk; RDSZ: recently diagnosed schizophrenia; ChSZ: chronic schizophrenia.

3.1.3. *RDSZ vs. controls*

The RDSZ group showed seven clusters of GM reduction involving both cortical and subcortical regions with total altered GM volume of 8,360 mm^3. ALE maxima were found in the: (a) left precentral gyrus (L-PrCG, BA 6), (b) left inferior frontal gyrus (L-IFG, BA 47), (c) bilateral superior temporal gyrus (STG, BA 22), (d) bilateral transverse temporal gyrus (TTG, BA 41), (e) right middle temporal gyrus (R-MTG, BA 21), (f) bilateral insular cortex (BA 13), (g) bilateral ACC (BA 32), (h) left parahippocampal gyrus (L-PHG, BA 34), and (i) left amygdala (L-Amy).

3.1.4. *ChSZ vs. controls*

Patients of the ChSZ group differed from HC in GM reduction in several cortical and subcortical regions grouped into seven clusters with a total altered GM volume of 14,912 mm^3. ALE maxima were found in the: (a) right medial frontal gyrus (R-MFG, BA 11), (b) L-IFG (BA 47), (c) L-STG (BA 22), (d) bilateral anterior insula (AI, BA 13), (e) bilateral ACC (BA 32/25), (f) bilateral amygdala, (g) head of the left caudal nucleus (L-Caud) and (h) medial dorsal nucleus (MDN) of the left thalamus (L-Thal).

3.2. *Between-groups comparisons and conjunction analyses*

Results of contrast and conjunction ALE analyses are shown in Table 2 and Fig. 5.

3.2.1. *c-HR vs. RDSZ*

c-HR U RDSZ: the conjunction analysis of c-HR and RDSZ groups showed a significant convergence of GM reductions in the R-ACC (BA 32) with a volume of common GM reduction of 144 mm^3.

c-HR < RDSZ: in the between-group comparison there were not significant GM reduction present exclusively in the c-HR as compared to the RDSZ group.

RDSZ < c-HR: contrariwise, there were significant reductions in four clusters regarding the RDSZ group as compared to the c-HR group. The total GM volume altered exclusively in the RDSZ group was 2,600 mm^3 with ALE maxima located in the left hemisphere, principally in cortical areas in the frontal lobe: (a) in the L-IFG (BA 44) and (b) in the L-PrCG (BA 4); (c) in the left postcentral gyrus (L-PoCG, BA 43); (d) in the L-STG (BA 22); in (e) the L-AI (BA 13) and (f) in the left claustrum (L-Clau).

Table 1
Clusters of gray matter reduction derived from the Anatomical Likelihood Estimation (ALE) analyses. For each cluster obtained, cluster size (mm^3), extrema ALE values, anatomical labels of the peaks of probability and their Talairach brain atlas coordinates were provided.

Cluster #	Volume (mm^3)	Talairach Daemon Label (Brodmann's Area)	Extrema Value	Talairach		
				x	y	z
g-HR < HC						
No cluster found						
c-HR < HC (tot. 800 mm^3)						
1	800	Right Anterior Cingulate Cortex (BA 32)	0.016	4	36	−6
RDSZ < HC (tot. 8,360 mm^3)						
1	1,776	Left Precentral Gyrus (BA 6)	0.025	−48	−10	24
		Left Inferior Frontal Gyrus (BA 44)	0.024	−48	4	18
2	1,624	Right Transverse Temporal Gyrus (BA 41)	0.025	48	−24	16
		Right Middle Temporal Gyrus (BA 21)	0.018	54	−26	−2
3	1,296	Right Middle Temporal Gyrus (BA 22)	0.023	50	−8	−8
		Right Insula (BA 13)	0.022	40	−10	−6
4	1,096	Left Insula (BA 13)	0.031	−32	22	4
5	1,032	Left Transverse Temporal Gyrus (BA 41)	0.024	−46	−18	10
		Left Superior Temporal Gyrus (BA 22)	0.020	−52	−8	6
6	784	Left Anterior Cingulate (BA 32)	0.022	−2	34	−4
		Right Anterior Cingulate (BA 32)	0.020	2	40	2
7	752	Left Amygdala	0.023	−20	−4	−18
		Left Parahippocampal Gyrus (BA 34)	0.015	−12	0	−14
ChSZ < HC (tot. 14,912 mm^3)						
1	4,928	Left Insula (BA 13)	0.042	−34	18	6
		Left Superior Temporal Gyrus (BA 22)	0.035	−48	4	2
		Left Insula (BA 13)	0.027	−44	12	0
		Left Inferior Frontal Gyrus (BA 47)	0.020	−40	20	−6
2	3,056	Right Insula (BA 13)	0.037	40	14	2
		Right Insula (BA 13)	0.035	32	18	8
3	2,312	Left Thalamus (Medial Dorsal Nucleus)	0.036	−2	−16	6
4	1,656	Right Medial Frontal Gyrus (BA 11)	0.032	4	36	−14
		Right Anterior Cingulate (BA 32)	0.031	4	32	−6
5	1,224	Left Caudate (Nucleus Head)	0.036	−4	6	−4
6	1,056	Left Amygdala	0.036	−20	−6	−12
7	680	Right Amygdala	0.026	16	−4	−16

g-HR: genetic high-risk; c-HR: clinical high-risk; RDSZ: recently diagnosed schizophrenia; ChSZ: chronic schizophrenia; HC: healthy controls.

3.2.2. RDSZ vs. ChSZ

RDSZ U ChSZ: the conjunction analysis of RDSZ and ChSZ groups showed five significant clusters of convergence of GM reductions in the left hemisphere (total volume of common GM reduction: 1,184 mm^3), namely (a) the L-PrCG (BA 6) and (b) the orbital part of the L-IFG (L-IFG, BA 44) in the frontal pole, (c) the L-AI (BA 13), (d) the L-ACC (BA 32), extending to right ACC and (e) the L-Amy.

RDSZ < ChSZ: in the between-group comparison there were three clusters of significant reduction regarding the RDSZ group as compared to the ChSZ group (total volume of altered GM present exclusively in the RDSZ: 672 mm^3), with ALE maxima located in the: (a) L-IFG (BA 44), (b) L-PrCG (BA 6), (c) L-PoCG (BA 43), (d) L-AI (BA 13); and right temporal lobe (e) in the R-MTG (BA 21). ChSZ < RDSZ: conversely, ChSZ group as compared to RDSZ group showed significant GM decreases in five clusters (total volume of altered GM present exclusively in the ChSZ: 1,464 mm^3) with ALE maxima located both in the left and right hemispheres in cortical and sub-cortical encephalic regions. In particular, ChSZ specific peaks of alteration were found in the: (a) L-IFG (BA 44), (b) L-STG (BA 22); (c) in bilateral AI (BA 13), (d) R-PHG (BA 34), (e) the right uncus (R-Unc, BA 34); (f) MDN and (g) pulvinar (Pulv) of the L-Thal, and (h) Pulv of the R-Thal.

3.3. Standard voxel-wise permutation tests

GM reductions in HR and SZ groups relative to HC are shown in **Table S6** and **Fig. S2**.

3.3.1. HR groups vs. controls

The g-HR group showed no significant cluster of variation. With regard to the c-HR group, a very small cluster was detected in the R-ACC.

3.3.2. SZ groups vs. controls

Overall, results reported statistically significant clusters largely overlapping with those identified by ALE. The RDSZ group showed eight clusters of GM reduction involving both cortical and subcortical regions with total altered GM volume of 2,246 mm^3. Maximum values were found in the: (a) L-IFG (BA 45), (b) L-AI (BA 13), (c) L-TTG (BA 41), (d) R-MTG (BA 22), (e) bilateral ACC (BA 32/24), and (f) L-PHG (BA 35). The ChSZ group showed eight clusters of GM reduction involving both cortical and subcortical regions with total altered GM volume of 17,913 mm^3. Maximum values were found in the: (a) L-MFG (BA 10), (b) bilateral AI (BA 13), (c) bilateral ACC (BA 32), (d) MDN of the L-Thal, and (e) bilateral PHG (BA 34), extending to the (f) amygdalar complex.

3.4. Behavioral characterization

Data-driven behavioral analysis revealed that aberrant ALE-derived patterns found in the clinical groups can be quantitatively associated with a wide range of functional neuroimaging tasks as shown in Fig. 6 and **Tables S7** (RDSZ group) and **S8** (ChSZ group).

We found no significant results associated with the R-ACC cluster in the c-HR group, whereas the whole-brain patterns of GM loss in the RDSZ and in the ChSZ groups were characterized by a statistically significant involvement of numerous different subdomains belonging to all five studied domains: cognition, perception, emotion, action and interoception. General distribution of the number of subdomains involved in each domain in the two clinical conditions is shown in the radar chart of Fig. 6. The ChSZ group, compared to the RDSZ group, displayed a higher number of involved subdomains (33 vs. 23). The main difference concerned the emotional domain with nine subdomains involved in the ChSZ group compared to the five of the RDSZ one. Fig. 6 (bottom panel) shows the ranking of the involved subdomains of the ChSZ group in decreasing order of z-score, coupled with the z-score of the corresponding subdomain in the RDSZ group. All the 23 functional subdomains found the RDSZ group were also present in the ChSZ group. The 10 subdomains exclusively associated with the GM loss in the ChSZ group were negative emotions (i.e. sadness, anger, unspecified negative emotions), positive emotions (i.e. happiness and unspecified positive emotions) of the emotion domain; "social cognition" and "memory" of the cognitive domain; "olfaction" of the perceptive domain; "inhibition of movement" of the action domain; and "sexuality (libido)" of the interoception domain.

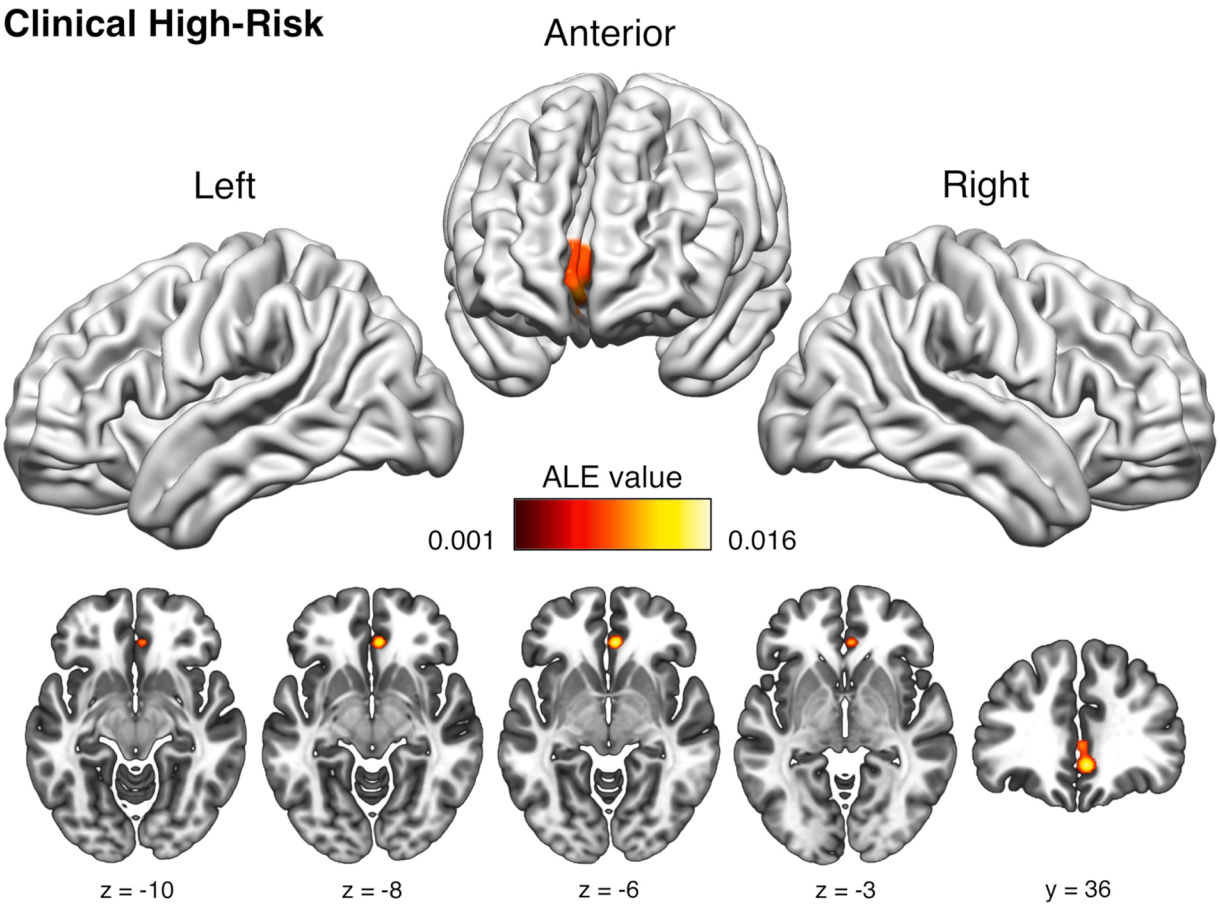

Fig. 2. Brain clusters of convergent GM reduction in the clinical high-risk (c-HR) group compared to healthy controls (HC). Results are FWE-corrected at .05 with cluster-forming value at $p < .001$. The ALE maps are visualized as three hemispheric surfaces (3-D cortical view) and five axial slices (2-D cortical and subcortical view). Brain templates are in neurological convention (i.e. R is right, L is left).

Subdomains associated with single ALE-derived clusters are represented in **Fig. S3** (RDSZ group) and in **Fig. S4** (ChSZ group). Of the seven ALE-derived clusters of GM reduction found in both the RDSZ and ChSZ groups, five clusters in each clinical group were significatively associated with at least one functional subdomain. In the RDSZ condition, the L-IFG was principally associated with action subdomains, bilateral TTG with perceptive subdomains, L-Ins with cognitive and action subdomains, and the L-Amy with emotional sub-domains. In the ChSZ group, bilateral insulae were principally associated with cognitive (including social cognitive), perceptive, action and interoceptive subdomains, L-Amy with emotional and perceptive sub-domains, L-Thal with cognitive subdomains and the L-Caud with reward/gain positive emotion subdomain.

3.5. Network decomposition

The results of the functional network decomposition analysis are shown in Fig. 7 and in **Table S9**. Fig. 7 (**A** and **B** panels) shows the subdivision of the morphometric alteration of the clinical groups into the different functional networks, while Fig. 7**C** depicts the percentage of altered GM volume in each network (i.e. proportional to the total altered GM volume in each clinical group).

In the c-HR group the ALE-derived cluster of GM alteration belonged to (a) the orbitofrontal cortex network - OFC-N (548 mm^3, 68.5 % of the total altered volume) and to (b) the salience network - SN (252 mm^3, 31.5 %). Most of the altered GM volume of the RDSZ fell within (a) the SN (2710 mm^3, 32.4 %), (b) the OFC-N (1217 mm^3, 14.6 %), (c) the left ventral attention network - L-VAN (1198 mm^3, 14.3 %), (d) the motor network - MN (1115 mm^3, 13.3 %), and (e) the sensorimotor network - SMN (932 mm^3, 11.2 %). In the ChSZ the most involved networks were: (a) the SN (4956 mm^3, 33.2 %), (b) the OFC-N (3971 mm^3, 26.6 %), and (c) the thalamus/basal nuclei network - Th-BN-N (2667 mm^3, 17.9 %).

3.6. Effects of meta-regression on GM reduction

Linear associations between selected clinical and methodological variables and VBM data of the included experiments of the whole SZ group are shown in **Fig. S5** (lower panel), **Tables S10** (demographic and clinical variables) and **S11** (methodological variables) and summarized as follows. As expected, the ALE results related to the whole SZ group were very similar in terms of spatial convergence with those of the AES-SDM (**Fig. S5,** upper panel). Voxel-wise correlation (i.e. Pearson's *r*) between the unthresholded ALE and AES-SDM z-score maps was $r = .64$ (calculated excluding the non-brain voxels).

3.6.1. Effects of demographic and clinical variables

Effect of sex: experiments with higher percentage of male patients were associated with a widespread GM loss in the: (a) L-STG ($p = 1.0e\text{-}5$, 52 voxels); (b) left inferior temporal gyrus (L-ITG; $p = 1.0e\text{-}4$, 46 voxels); (c) R-Ins ($p = 6.0e\text{-}5$, 50 voxels); (d) bilateral thalami ($p = 5.0e\text{-}6$, 94 voxels).

Effect of antipsychotic treatment: in experiments with higher percentage of medicated patients compared with studies with a higher percentage of drug-naïve patients at the scan time, we found a more widespread decrease of the GM volumes of (a) the L-MFG ($p = 2.0e\text{-}4$, 39 voxels) and of (b) the R-STG ($p = 2.0e\text{-}5$, 127 voxels).

Antipsychotic dosage, age at scan and positive and negative symptoms: no linear associations with age at scan, medication dosage

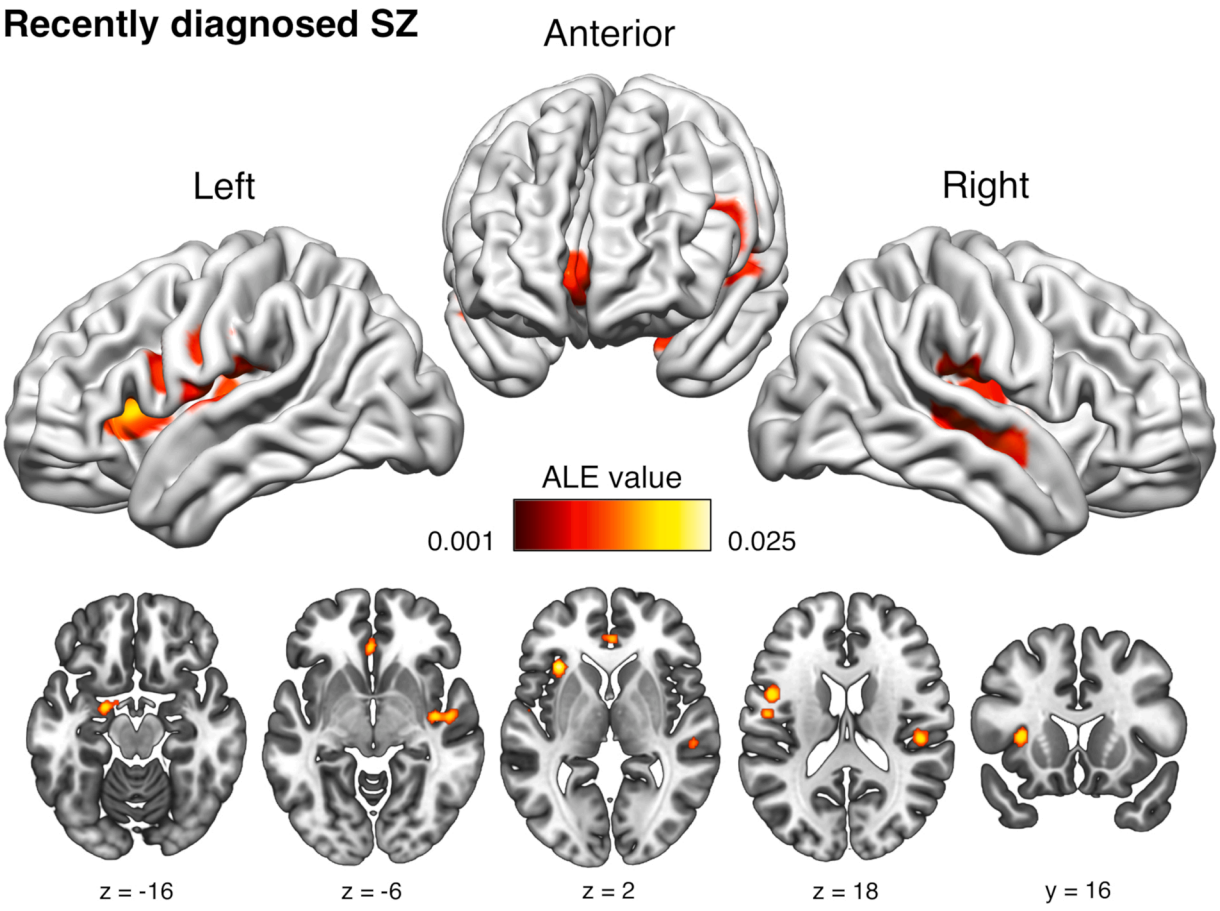

Fig. 3. Brain clusters of convergent GM reduction in the recently diagnosed schizophrenia (RDSZ) group compared to healthy controls (HC). Results are FWE-corrected at .05 with cluster-forming value at $p < .001$. The ALE maps are visualized as three hemispheric surfaces (3-D cortical view) and five axial slices (2-D cortical and subcortical view). Brain templates are in neurological convention.

(chlorpromazine mg equivalents), positive and negative symptoms (PANSS positive and negative scores) were found.

3.6.2. Effects of methodological variables

Sample size: experiments with smaller sample size showed a more widespread GM decrease volume in (a) the right STG (R-STG), extending to (b) the R-Ins ($p = 4.0e-7$, 293 voxels) and in a small cluster located (c) in the L-ACC ($p = 1.0e-5$, 28 voxels).

Image smoothing level (FWHM): higher smoothing was significantly associated with GM reduction in (a) the R-Ins, extending to (b) the R-PrCG ($p = 1.0e-4$, 86 voxels) and in the (c) L-STG ($p = 1.0e-4$, 27 voxels).

Field strength and slice thickness: linear associations with VBM data and these variables were not found.

4. Discussion

By reviewing a vast literature of voxel-based neuroimaging studies about schizophrenia, this meta-analysis offers the most overarching picture of morphometric changes of GM currently available and lends support to pathophysiological models, which combine progressive brain alterations with the clinical evolution of SZ. Using a conservative study selection and the current state-of-the-art methods in the CBMA field, we have identified GM alterations associated with clinical high-risk subjects, recently diagnosed and chronic patients with SZ, providing meta-analytical evidence of progressive brain morphometric changes after prodromal symptoms and signs onset. As a distinguishing feature of this study, we have established an objective link between the SZ symptomatology and the underlying neural pathophysiology, associating the resulting GM changes with data-driven functional profile characterizations. Our findings also demonstrate between-study effects of sex, sample size and medication on published VBM results.

4.1. GM alterations partly reproduce previous CBMA results on SZ stages

Our findings are only in part consistent with those of the previous meta-analyses on the different stages of SZ, providing new important information about the progression of GM alteration during the course of the disorder. Interestingly, our analyses showed that there were no morphometric differences between g-HR and HC groups. This result is in line with a recent CBMA of VBM studies on first degree relatives of patients with SZ (Saarinen et al., 2020), but not with previous investigations reporting GM tissue loss at the level of the R-ACC and L-PHG (Fusar-Poli et al., 2011a, 2014). The lack of significant findings may be explained by a variety of factors. For example, as early meta-analytic syntheses have been published with significant smaller data sets (i.e. less than 10 VBM experiments each) due to the limited availability of research data, our results are particularly robust and reasonably non-driven by singly experiments (Eickhoff et al., 2016). It is worth noting that the mean age at the scan of the first/second degree relative varies widely across experiments (**Table S2**), which increases the between-study variability. Also, it has been suggested that specific morphometric brain variations in g-HR subjects may be present only in those who develop psychosis later in life (Smieskova et al., 2010, 2013). However, as these subjects represent a small portion of the g-HR population (Fusar-Poli et al., 2012), their contribution could be covered by the substantial number of the non-transitioning subjects.

Regarding c-HR group, we confirmed the GM loss in the R-ACC found in previous CBMAs (Chan et al., 2011; Fusar-Poli et al., 2011a).

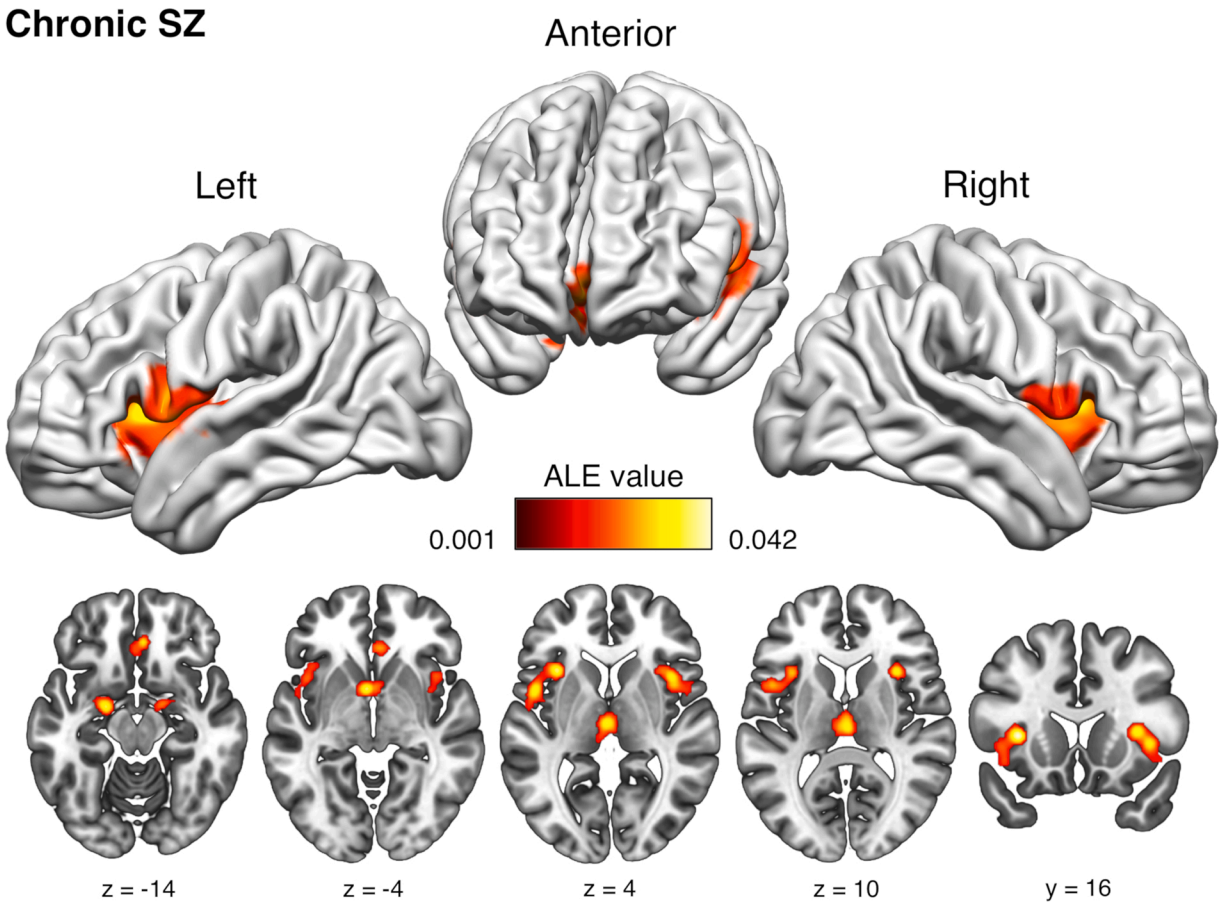

Fig. 4. Brain clusters of convergent GM reduction in the chronic schizophrenia (ChSZ) group compared to healthy controls (HC). Results are FWE-corrected at .05 with cluster-forming value at $p < .001$. The ALE maps are visualized as three hemispheric surfaces (3-D cortical view) and five axial slices (2-D cortical and subcortical view). Brain templates are in neurological convention.

However, the R-AI, L-Amy and L-IFG clusters found by Chan et al. (2011), and the R-STG, L-PHG, L-AI, R-IFG ones found by Fusar-Poli et al. (2011a) have not survived our rigorous thresholding procedure. Moreover, unlike early meta-analyses (Boos et al., 2007), we have not replicated the hippocampal reduction in HR groups, probably due to our whole-brain approach, which has selectively excluded studies using ROI or SVC analyses on this region (McDonald et al., 2008).

In the RDSZ group, we confirmed the findings that the L-IFG, L-Amy and bilateral ACC show GM decreases (Chan et al., 2011; Ellison-Wright et al., 2008), but not the findings of GM reduction in the caudate, thalamus and cerebellum. In this group, we have also revealed GM alterations in the temporal cortices, bilateral insula and L-PHG, which were associated with ChSZ patients only in those previous investigations. For what concerns the ChSZ group, we confirmed the presence of bilateral GM alterations in the AI, ACC, and amygdala. The left IFG was also found by early CBMAs (Chan et al., 2011; Ellison--Wright et al., 2008). Furthermore, we revealed a cluster of GM reduction in the bilateral thalamus, which was only left-lateralized in Chan et al. (2011), and in the left caudate head, which was not found in the previous ALE studies. It should be noted that the involvement of the aforementioned regions in SZ groups was confirmed by the standard voxel-wise permutation tests. Taking this into account, it is reasonable to assume that our state-of-the-art multiple-comparison corrections ensure an adequate type I error control than the liberal (but previously employed) FDR correction, as the latter is prone to reveal false positive findings in meta-analytic neuroimaging investigations (Eickhoff et al., 2016, 2017; Müller et al., 2017; Nani et al., 2019; Samea et al., 2019).

Another important result of the present work that contrasts with previous ALE investigations (Chan et al., 2011; Ellison-Wright and Bullmore, 2010; Fornara et al., 2017; Fornito et al., 2009) is the systematic absence of the lingual and fusiform gyri, cuneus, posterior cingulate and cerebellum in the SZ clinical groups. As to this aspect, we note that these posterior areas were found altered in a relatively small number of included studies. Therefore, the discrepancy may be due to the fact that our statistical inference was more sensitive to large effects, and less affected by individual experiments (Eickhoff et al., 2017, 2016). Finally, our results fit well with findings of white matter (WM) degeneration. In previous studies (Bora et al., 2011; Vitolo et al., 2017) the anterior part of the corpus callosum, the anterior thalamic radiation, inferior longitudinal and fronto-occipital fasciculi, cingulate bundle and fornix were associated to SZ. Notably, these tracts connect GM regions that have been found to be decreased in at least one of the stages. For instance, the anterior corpus callosum might contribute to abnormalities in interhemispheric communication between the AIs during the progression of the disorder, in agreement with studies reporting volumetric alteration of right deep prefrontal-insular WM and a widespread disruption of right genu of the corpus callosum in ChSZ individuals (Mitelman et al., 2009; Spalletta et al., 2015; Sugranyes et al., 2012). To note, long association tracts connecting bilateral ACC, AI and medial prefrontal cortex have been found altered in SZ (Bora et al., 2011; Reid et al., 2016), and also the aberration of bilateral anterior thalamic radiation is a well-replicated finding in chronic stage of the disease (Canu et al., 2015; Li et al., 2017). Taken in this context, GM findings of the present study are in line with fronto-striatal and temporo-limbic systems disruption as well as evidence regarding progressive disconnection of the brain in SZ.

Table 2
Clusters of gray matter difference and conjunction derived from the Anatomical Likelihood Estimation (ALE) analyses. For each cluster obtained, cluster size (mm^3), extrema values, anatomical labels of the peaks of probability and their Talairach brain atlas coordinates were provided.

Cluster #	Volume (mm^3)	Talairach Daemon Label (Brodmann's Area)	Extrema Value	Talairach		
				x	y	z
c-HR U RDSZ (tot. 144 mm^3)						
1	144	Right Anterior Cingulate Cortex (BA 32)	0.014	2	36	−6
c-HR < RDSZ						
		No cluster found				
RDSZ < c-HR (tot. 2,600 mm^3)						
1	1,032	Left Superior Temporal Gyrus (BA 22)	p < .001	−50.2	−13.3	8.4
		Left Insula (BA 13)	p < .001	−47.3	−18.7	16
2	768	Left Postcentral Gyrus (BA 43)	p < .001	−50	−10	16
		Left Precentral Gyrus (BA 4)	p = .001	−51.6	−12	24.4
3	576	Left Insula (BA 13)	p = .001	−32	12	8
		Left Insula (BA 13)	p = .002	−36	13	5
		Left Claustrum	p = .005	−30	18	2
		Left Inferior Frontal Gyrus (BA 45)	p = .009	−32	24	6
4	224	Left Insula (BA 13)	p = .002	−46	4	14
		Left Inferior Frontal Gyrus (BA 44)	p = .003	−49.5	1	15.5
RDSZ U ChSZ (tot. 1,184 mm^3)						
1	680	Left Insula (BA 13)	0.029	−32	20	4
2	304	Left Amygdala	0.023	−20	−4	−16
3	120	Left Anterior Cingulate (BA 32)	0.020	0	34	−4
4	56	Left Precentral Gyrus (BA 6)	0.018	−52	−6	6
5	24	Left Inferior Frontal Gyrus (BA 47)	0.016	−48	6	14
RDSZ < ChSZ (tot. 672 mm^3)						
1	520	Left Precentral Gyrus (BA 6)	p = .001	−49	−5	24.4
		Left Postcentral Gyrus (BA 43)	p = .002	−50	−8.5	17.5
		Left Inferior Frontal Gyrus (BA 44)	p = .004	−49	0	20
2	136	Left Postcentral Gyrus (BA 43)	p = .006	−47	−17	14
		Left Insula (BA 13)	p = .007	−46	−14	10
3	16	Right Medial Temporal Gyrus (BA 21)	p = .006	44	−8	−12
ChSZ < RDSZ (tot. 1,464 mm^3)						
1	672	Right Parahippocampal Gyrus (BA 34)	p < .001	12.8	−3.6	−16
		Right Uncus (BA 34)	p = .001	17.7	−4.4	−19
2	480	Left Thalamus (Medial Dorsal Nucleus)	p = .001	−7	−20	11
		Right Thalamus (Pulvinar)	p = .002	4	−24	9
		Left Thalamus (Pulvinar)	p = .003	−3.5	−23	4.5
3	256	Left Precentral Gyrus (BA 44)	p = .001	−46	12	8
		Left Insula (BA 13)	p = .005	−44	0	2
4	40	Right Insula (BA 13)	p = .003	36	20	2
5	16	Left Superior Temporal Gyrus (BA 22)	p = .01	−51	8	4

g-HR: genetic high-risk; c-HR: clinical high-risk; RDSZ: recently diagnosed schizophrenia; ChSZ: chronic schizophrenia; HC: healthy controls.. <: Indicates that the gray matter (GM) reduction is wider in the group to the left of the symbol. U: indicates the clusters of GM volume reduction found in the groups both to the left and to the right of the symbol.

4.2. Differences and overlaps between clinical groups: evidence for a typical progression of the GM loss

While none of the meta-analytic works to date assessed an objective overlap estimation between the c-HR, RDSZ and ChSZ groups, here we have quantitatively evaluated the conjunction areas of alteration, in parallel with the differential areas emerging from the between groups comparisons. The contrast ALE analyses showed that the RDSZ group report a larger brain volume characterized by GM reduction compared to c-HR group, suggesting an important enlargement of altered encephalic areas during the first period of full-blown non-affective psychosis. We found a similar trend in the second comparison: recently diagnosed versus chronic SZ. In this case, the two groups differ significantly for mean age, duration of illness and for the total volume of GM decrease (Tables 2 and **S4**).

The strong increment in the GM reduction found in the post-onset phase of SZ may be explained by the fact that the c-HR groups include heterogeneous subclinical psychopathological states that not necessarily, and in a relatively small proportion (approximately 36 % after 3 years from the first evaluation), will transition into a diagnosis of SZ (Falkenberg et al., 2015; Fusar-Poli et al., 2012). In addition, the first months after the onset of the disorder are considered the most critical in influencing prognosis and the most correlated to neurotoxic processes, especially if the patient is not correctly and promptly diagnosed and treated (Anderson et al., 2014).

The R-ACC is the only cluster found among c-HR subjects and is also present in the SZ groups, suggesting a potential significant role of this area in the development and progression of the disorder. Both structural and functional aberrations of the R-ACC are well-replicated findings in different cohorts of individuals at high clinical-risk for psychosis (Allen et al., 2010; Fornito et al., 2008; Fusar-Poli et al., 2011a, b; Fusar-Poli et al., 2014; Jessen et al., 2006; Shim et al., 2010; Takayanagi et al., 2017). Moreover, this anatomical region was recently proposed as being the epicenter of neuronal volume loss in SZ (Shafiei et al., 2020). Therefore, the ACC volumetric loss could represent a neuroimaging marker of SZ both before (that is, in the prodromal phase with a putative prognostic significance of transition to SZ) and after the onset of the disorder. However, further research is needed to unravel this issue, especially on patients who later develop psychosis and with the help of harmonized longitudinal protocols to increase comparability across

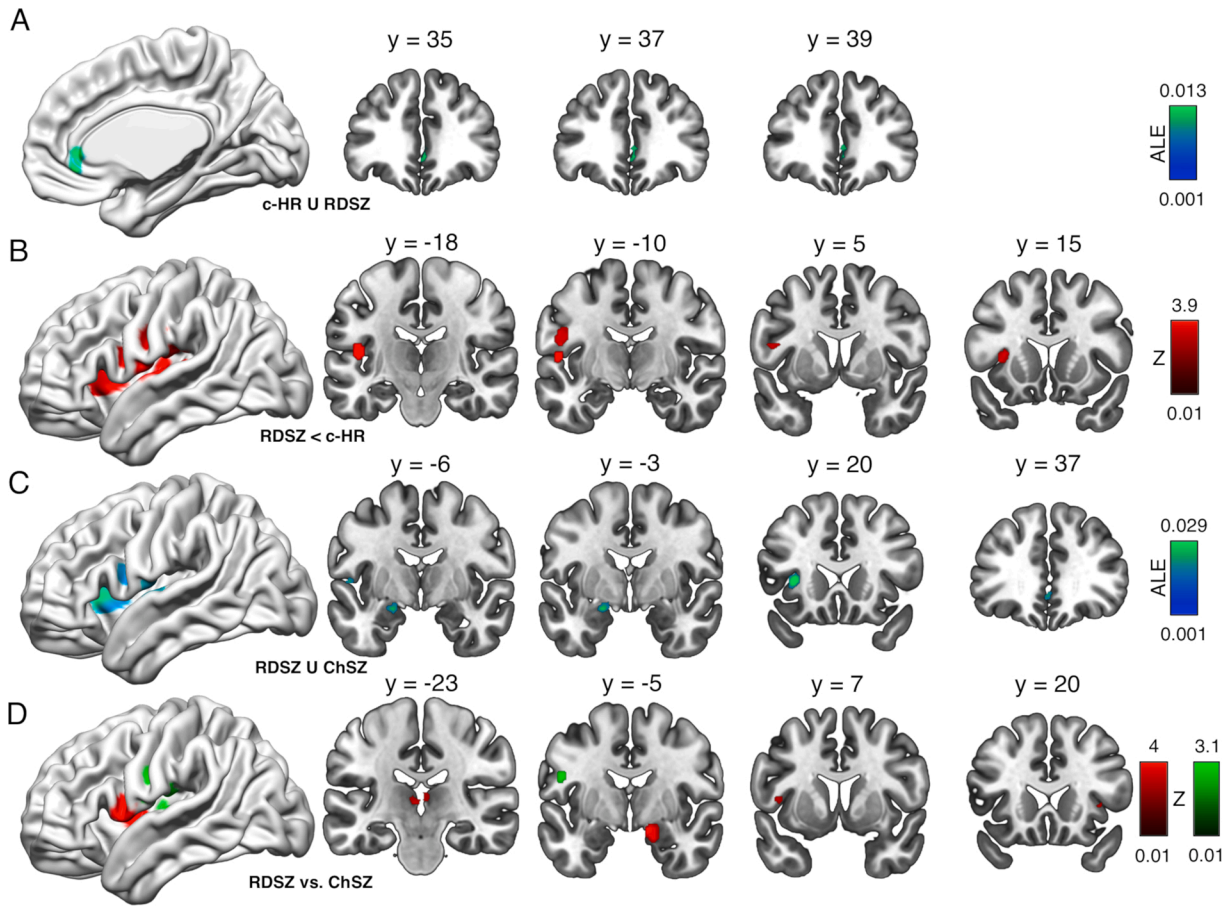

Fig. 5. Conjunction and contrast analyses between clinical groups. (A) Convergence of GM reduction between clinical-high risk and recently diagnosed schizophrenia groups (colors from dark to light blue represent increasing ALE values). (B) Compared to the clinical-high risk group, GM reductions are exclusively present in the recently diagnosed schizophrenia patients (colors from dark to light red represent increasing z-point values). (C) Convergence of GM reduction between recently diagnosed and chronic schizophrenia groups (colors from dark to light blue represent increasing ALE values). (D) Compared to the chronic schizophrenia group, GM reductions are exclusively present in the recently diagnosed patients (colors from dark to light green represent increasing z-point values). Compared to the recently diagnosed schizophrenia group, GM reductions are exclusively present in the chronic patients (colors from dark to light red represent increasing z-point values). ALE results were computed using a p value $< .01$ and minimum cluster-size > 10 mm^3.

multiple sites (Andreou and Borgwardt, 2020; Cannon et al., 2014; Fusar-Poli et al., 2012).

When compared to the c-HR group, the RDSZ condition shows 4 leftward clusters of higher GM reduction, located in the frontal, parietal, temporal, insular cortices and in the subcortical region of the claustrum (Table 2). These results suggest a typical diffusion of GM decrease across left hemispheric cortical areas, which can be detected in the first months after the onset of the disorder (Takahashi and Suzuki, 2018). Interestingly, our findings align with both theoretical and experimental proposals suggesting a prominent abnormal left asymmetry of neural systems in SZ driven by volumetric reductions (Oertel et al., 2010; Oertel-Knöchel and Linden, 2011; Ribolsi et al., 2014). The cortical involvement of the left hemisphere in early stages of SZ was also described by recent resting-state functional connectivity MRI studies (Li et al., 2019c, 2017; Wang et al., 2019), which outlined a prevalence of reduced leftward interactions between the functional networks involved in language, interoceptive awareness, auditory and sensory processing. Furthermore, the volumetric reduction of highly connected anatomical structures (such as the AI, STG, IFG and claustrum) is consistent with the pathophysiological model proposed by Palaniyappan (2017), according to which a GM dysfunctional remodeling takes place in topologically important hubs of the brain, mostly in the immediate post-onset phase of SZ, thus representing an adaptive but inefficient compensatory response to the disorder itself.

RDSZ and ChSZ conditions share convergent patterns of volumetric GM loss preferentially in the left hemisphere (i.e. IFG, PrCG, AI and Amy), except for the bilateral cluster of ACC (Fig. 5). These higher-order integration areas were repeatedly found altered in both the recently diagnosed and chronic populations, and related to the wide range of signs and symptoms of SZ (Jeong et al., 2009; Killgore et al., 2009; Shepherd et al., 2012; Wylie and Tregellas, 2010; Yan et al., 2012). It is worth noting that these regions partially overlap with the cortical distribution of the Von Economo Neurons (VENs), large spindle-bipolar neuronal cells, mostly located in layer V of the AI and of the ACC (Allman et al., 2010, 2011). VENs are also present in great apes and other mammalians and are associated with "social brain" abilities (Butti et al., 2013; Cauda et al., 2014). Alterations of this neuronal subpopulation in post-mortem histological studies were associated with SZ (Brüne et al., 2010, 2011; Krause et al., 2017). Overall, results are to be interpreted with caution as these neuroanatomical regions were also recently classified as brain hubs with *high structural alteration variety*, which is to say that they can be affected by a wide range of psychiatric and neurological disorders (Cauda et al., 2019; Crossley et al., 2014; Liloia et al., 2018). Following this view, the development of 'reverse inference' methodologies (e.g. advanced computational tools based on Bayesian statistic inference) is needed to better define neural substrates that are specific to SZ.

Contrast analyses between SZ groups highlight the presence of areas of volumetric loss, which are specific to either the recent diagnosis or to the chronic conditions. A selective GM reduction, found in the RDSZ

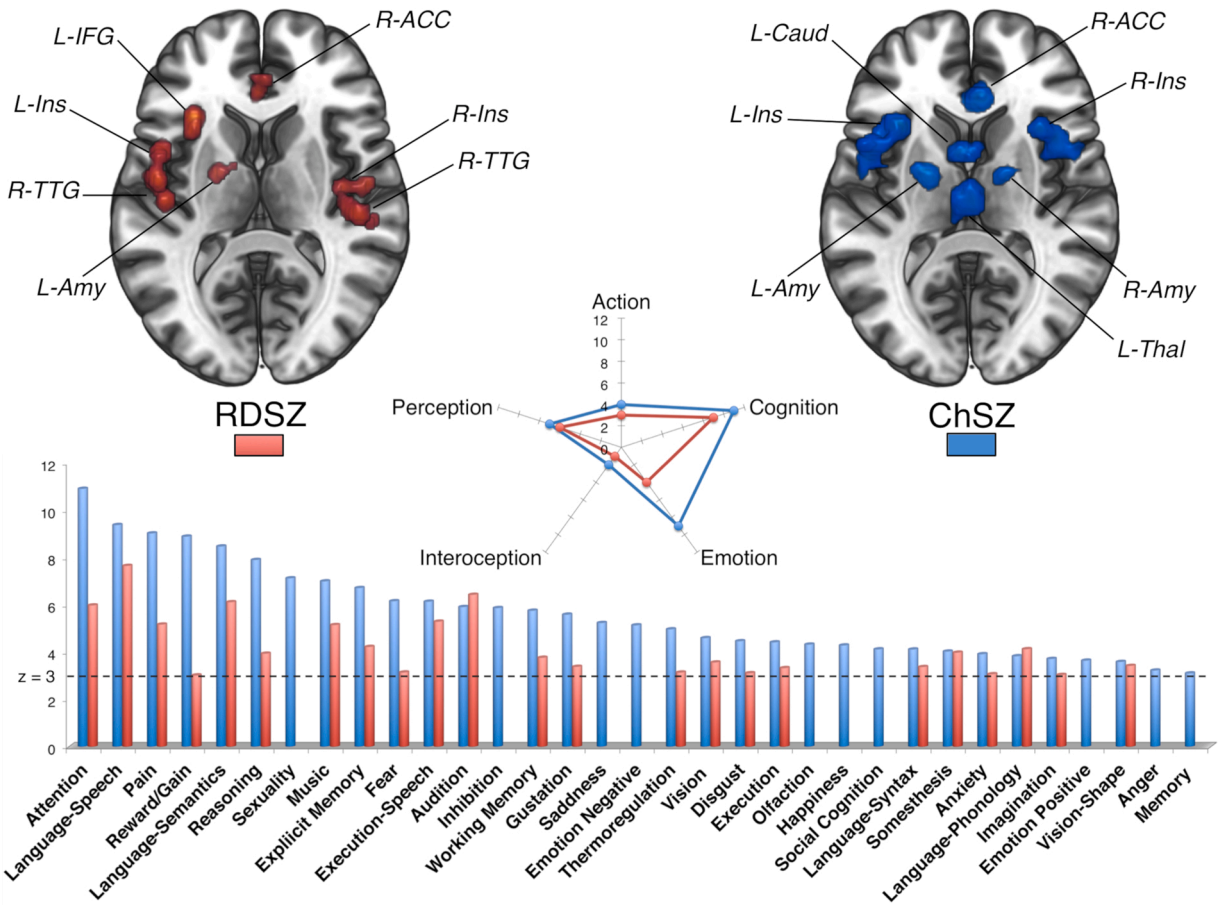

Fig. 6. Behavioral characterization results of whole ALE-derived brain maps of GM reduction obtained in the RDSZ and ChSZ groups. (Upper panel) Alteration patterns are visualized as two axial slices (3-D cortical and subcortical view). (Central panel) Number of subdomains significantly associated in each domain. (Bottom panel) Z-scores of significant subdomains. A threshold of $p < .05$ with Bonferroni correction for multiple comparisons was applied, corresponding to a subdomain z-scores ≥ 3.

GM: gray matter; ACC: anterior cingulate cortex; Ins: insula; IFG: inferior frontal gyrus; TTG: transverse temporal gyrus; Amy: amygdala; Caud: caudate; Thal: thalamus.

group only, belongs to cortical areas of the frontal, parietal and insular lobes of the left hemisphere and, to a lesser extent, to the right temporal lobe. The leftward temporal and prefrontal clusters observed in the RDSZ patients might suggest some form of dysfunctional compensation or reorganization mechanism that might take place just after the disruption caused in the acute phase of the first episode of psychosis (Palaniyappan, 2017).

In the ChSZ group five clusters of more marked GM reduction have been found in both cerebral hemispheres, showing a left-to-right and cortical-to-subcortical enlargement that appears to affect the bilateral AI, PHG, Amy, Thal (pulvinar and medial dorsal nuclei) and the STG. This robust finding is significant, given that GM reductions occurring homotopically have been underemphasized by previous voxel-based investigations. It also worth noting that both cross-sectional and longitudinal approaches have so far collected conflicting results for parahippocampal and amygdalar involvement at different phases of SZ (Shepherd et al., 2012). In accordance with some studies (Asami et al., 2012; Chan et al., 2011; Davidson and Heinrichs, 2003; Velakoulis et al., 2000; Wright et al., 2000), our results underline that abnormalities of the left amygdala-parahippocampal complex are present during the first stages of SZ and that the involvement of the right complex is likely to reflect the chronicity of the disorder. Furthermore, recent studies reported a disrupted interhemispheric coordination in terms of altered functional connectivity and white matter tracts in subjects with SZ (Hoptman et al., 2012; Liu et al., 2018; Sun et al., 2015). Interestingly, new lines of research support the idea that GM tissue damage in SZ is constrained by brain pathways (Cauda et al., 2018; Shafiei et al., 2020), and intimately related to homotopic interactions (Mancuso et al., 2019). These findings emphasize the role of aberrant connections linking homotopic areas in the development of SZ.

Although thalamic anomalies are well known to be implicated in the SZ condition (Pergola et al., 2015), some meta-analytical investigations found significant volumetric reductions of this diencephalic structure starting from the early phase of illness (Adriano et al., 2010; Ellison--Wright et al., 2008), and others in the chronic stage only (Bora et al., 2011) or exclusively left-lateralized in ChSZ (Chan et al., 2011). This inconsistency is not entirely surprising: different results could be due to the limited MRI resolution, heterogeneity in meta-data selection, study design, as well as to different methodological procedures. The present ALE meta-analysis highlights a selective involvement of L-MDN and bilateral pulvinar in the ChSZ condition, which accords well with some neuroimaging and post-mortem studies (Brickman et al., 2004; Byne et al., 2001, 2009; Horga et al., 2011; Kemether et al., 2003; Pergola et al., 2015; Shimizu et al., 2008).

Even if the neurobiological agents underlying these changes remain largely unknown and the role of structural and functional connectivity in the GM progression is still an open issue in SZ and other neuropsychiatric disorders (Cauda et al., 2019), the marked increase of the GM volume reduction found in the three stages of the disorder here analyzed (c-HR < RDSZ < ChSZ) is consistent with the contemporary pathophysiological models of SZ, which describe altered neurodevelopmental long term processes accompanied by neuroprogression phenomena

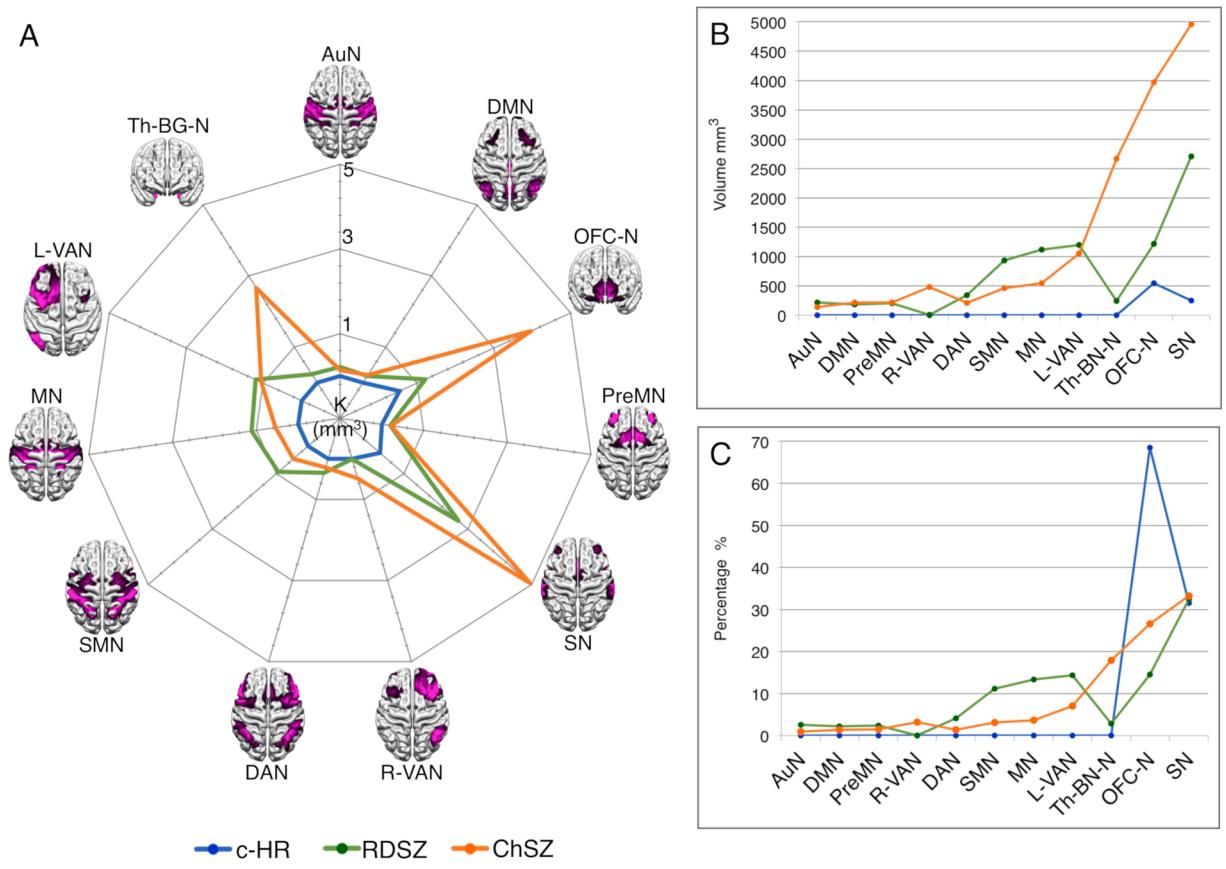

Fig. 7. Functional network decomposition of the ALE-derived clusters of GM reduction obtained in the c-HR, RDSZ and ChSZ groups. (A and B) Graphical representations of the number of altered volumes (mm^3) falling within a functional network. (C) Graphical representation of the altered volumes falling within a functional network (percentage).
AuN: auditory network; DMN: default mode network; preMN: premotor network; R-VAN: right ventral attention networks; DAN: dorsal attention network; SMN: sensorimotor network; MN: motor network; L-VAN: left ventral attention networks; Th-BN-N: thalamus-basal nuclei subcortical network; OFC-N: orbito-frontal cortex network; SN: salience network.

(Andreasen, 2010; Ashe et al., 2001; Keshavan, 1999; Palaniyappan, 2017).

4.3. *Behavioral characterization: unbiased evidence for a link between GM alterations and psychological features of the disorder*

The progression of GM alteration from the RSDZ condition to the ChSZ one has its counterpart in the functional characterization, as all the behavioral subdomains found in the RDSZ group are shared by the ChSZ subjects, who show many other involved mental processes.

Auditive perceptive and phonologic linguistic subdomains exhibit the higher z-scores in the RDSZ condition. The GM reduction associated with the auditive alteration is in agreement with a higher prevalence of positive symptoms in the first months after the onset of the disorder, such as paracusia (Fountoulakis et al., 2019, 2020), while the phonologic linguistic involvement may be lead to the negative symptoms affecting language processes (Compton et al., 2018). Among these symptoms, aprosody, a specific aspect of the vocal blunted affect, defined as the reduced ability to produce the melodic line of speech thanks to variations in pitch, rhythm, and stress of pronunciation, has been recently associated with patients with a shorter DOI (Compton et al., 2018). Focusing on GM alteration at a single cluster-level in RDSZ, we find the involvement of linguistic and action speech subdomains associated with the GM reduction in the L-IFG cluster, and of perceptive subdomains (audition and pain) connected with the bilateral TTG clusters. The L-IFG is considered a central node of human brain, implicated in semantic and affective integration during communication (Belyk et al., 2017); its volumetric reduction and dysconnectivity in the first phases of SZ has been associated to linguistic, memory and encoding impairment (Bonner-Jackson et al., 2005; Chen et al., 2014; Jeong et al., 2009).

With regard to common subdomains shared by the two SZ groups, two clusters of GM reduction emerge: L-Ins and L-Amy. The L-Ins cluster suggests an involvement of several cognitive functions, including attention, reasoning, language, working and explicit memory and music comprehension, as well as of action subdomains like execution of speech and inhibition of movement. These data-driven associations accord well with the findings of Liao et al. (2015), who found positive correlations between the GM volume of the L-Ins and performance at the Digit Symbol Substitution Test (DSST; Jaeger, 2018) in a large cohort of patients with SZ.

To note, this region has been recently found to predict treatment response and clinical prognosis of both RDSZ and ChSZ patients (Li et al., 2019b; Mikolas et al., 2016), showing an important role in the pathophysiology of SZ. In both SZ groups, the L-Amy cluster was linked to negative emotional, explicit memory and visual perception functions. Functional MRI studies report aberrant amygdalar activation in SZ, showing patterns of hypo-connectivity with the insula and IFG during emotional and social recognition tasks (Mier et al., 2019; Mukherjee et al., 2014).

In ChSZ several mental processes, relating to neurocognition (i.e. attention and reasoning), language (i.e. speech and semantics), reward/gain positive emotion and sexuality (i.e. libido) show a high z-score at cluster-level. The neurocognitive impairment, especially the deficits in

attentional functions, is a typical trait of SZ (Green et al., 2019; Kahn and Keefe, 2013), which is present since the prodromal phase with important worsening at the illness onset and a slower increment during its progression (Seidman and Mirsky, 2017). In this regard, we observe that a previous voxel-based investigation of ChSZ subjects (Schiffer et al., 2010) showed significant associations between GM volume of frontal/-cingulate cortex and planning performance, reasoning, and executive inhibition.

The involvement of cognitive functions related to language production can partially explain the negative symptomatology of SZ, in particular some expression deficits like alogia, and aprosody (Compton et al., 2018). We suppose a similar correlation between the involvement of the reward/gain emotional processes and the pole of reduced motivation of the negative symptoms, interpreted as a product of the reduced ability to expect and feel pleasure during activities (anhedonia) and the reduced ability to start actions and projects (avolition) (Lee et al., 2015). The high engagement of emotional subdomains, defined as the "mental faculty of experiencing an affective state of consciousness" (http://brainmap.org/taxonomy/behaviors.html), including positive and negative emotion like reward/gain, happiness, fear, sadness, disgust, anxiety and anger, may represent a neuroanatomical counterpart of the blunted affect dimension of negative symptoms. More generally, the significant involvement in the ChSZ group of mental processes theoretically related to negative symptoms is concordant with the high prevalence of this type of symptoms in the chronic condition (Fountoulakis et al., 2019, 2020). Indeed, primary persistent negative symptoms still represent an unmet need in the care of patients with SZ (Mucci et al., 2017). Finally, the GM reduction of cerebral areas correlated with sexual interoception is in line with the evidence of deficits in sexual cognition and fantasy arousal found in unmedicated patients with SZ: these deficits, therefore, are not necessarily secondary to the antipsychotic treatment (Dembler-Stamm et al., 2018).

4.4. Functional networks and their relationship with different SZ stages

Most of the altered GM volume in each clinical group belongs to encephalic regions that are key nodes of the SN, which is composed by the ACC, the ventral part of the PrCG (BA 6, pre-SMA) and the AI (Seeley et al., 2007). The pivotal role played by this functional network in the psychopathology of SZ is supported by numerous studies that found associations between structural and functional alteration of the SN and the core symptoms and the prognosis of the disorder (Li et al., 2019b; Palaniyappan and Liddle, 2012). Moreover, in agreement with our results, alteration of the SN was found in all the SZ stages (Mallikarjun et al., 2018; Spreng et al., 2019; Wang et al., 2016). The SN is thought to be responsible for dynamic switching between default mode and task-related states of the brain, and is engaged in a plethora of tasks involving interoceptive, action, perceptive and cognitive domains (Menon and Uddin, 2010; Uddin, 2015). Our behavioral characterization accords well with this evidence.

In terms of absolute number of volumes associated, the OFC-N was the most functional network involved in the c-HR group, with the following progression between the three clinical groups: c-HR < RDSZ < ChSZ. The importance of the OFC-N in the prodromal phase of SZ was emphasized by Collin et al. (2018), who found that the OFC resting-state functional connectivity (rsFC) is a distinctive trait of the c-HR subjects that, after the MR scan, transition into overt psychosis. The OFC-N is involved in the inference of the expected outcomes' values. This inference ability is impaired when the rsFC of the OFC is reduced with targeted transcranial magnetic stimulation (Howard et al., 2020). Therefore, a GM decrease of OFC-N cortical areas could be related to the prodromal negative symptoms, particularly to the motivational deficits that are frequently found in c-HR subjects and heavily impact on quality of life (Glenthoj et al., 2020).

Morphometric variations of RDSZ appear to accumulate preferentially in specific functional systems, namely L-VAN, MN and SMN. GM reductions of the BA 44, 45 and 47 located in the L-IFG correspond to a selective involvement of the L-VAN, that is thought to be involved in reorienting attention toward unattended stimuli (Corbetta et al., 2002). This result accords well with the evidence of altered connectivity of the VAN in patients in the SZ early-stage (Hummer et al., 2020). However, it should be noted that the involvement of the R-VAN is almost exclusive to the ChSZ condition; it might therefore be considered as the functional counterpart of the homotopic progression (from left to right) of the GM alteration.

A significant GM decrease of the BAs 6 and 4, which are parts of the MN, is specifically found in the RDSZ condition. In particular, the primary motor area (M1) corresponds to the BA 4 and the premotor area (PMA), while the supplementary motor area (SMA) and the pre-SMA partly belong to the BA 6. Our findings are in agreement with previous studies showing alteration of M1 and SMA connectivity in SZ, after controlling for age and antipsychotic medications (Bernard et al., 2017), as well as alteration of the BA 6 correlated with abnormal involuntary movements in RDSZ patients (Kindler et al., 2019).

The specific GM reduction of the *pars opercularis* of the PoCG (BA 43), which constitutes part of the secondary somatosensory area (S2), corresponds to the selective involvement of the SMN found in the RDSZ group. This network is involved in auditory, visual, tactile and direct pain perception, social perception (observation of the stimulus perceptedby others), and empathetic accuracy tasks (judging the meaning of the social stimulus) (Keysers et al., 2010; Paracampo et al., 2017). The SMN dysconnectivity has been associated with multiple transdiagnostic dimensions of psychopathology in different major psychiatric disorders, including SZ (Kebets et al., 2019). Furthermore, a recent study on RDSZ subjects demonstrated how, in this specific phase of the disorder, sensorimotor conflictual stimuli could induce failure in bodily self-monitoring by generating presence hallucination, that is, by making patients wrongly perceive a person standing behind themselves (Salomon et al., 2020).

GM reductions in the bilateral thalami (MDN and pulvinar) and in the head of the left caudate have been specifically associated with the ChSZ group. In this group such GM loss may reflect the greater involvement of the Th-BN-N at both absolute and relative levels. This result is in line with a recent study on ChSZ patients (mean DOI > 15 years) that reported a hypo-connection of the SN with the MDN of the thalamus, the ventral parts of striatum and the pallidum, and a hyperconnection of the SMN with the anterior ventral nucleus of the thalamus and the dorsal striatum, which includes the caudate nucleus (Avram et al., 2018). Thus, according to this evidence and to our results, it is likely a progressive involvement of subcortical "relays" structures as SZ develops. This engagement might play a role in the dysconnectivity and altered integration of other functional networks, such as the SN, MN and the SMN (Ferri et al., 2018; Hua et al., 2019; Skåtun et al., 2018).

4.5. Effects of clinical and methodological variables

Our voxel-wise meta-regression approach suggests that gender, antipsychotics, sample size and imaging smoothing level had significant effects on GM alterations across experiments. The result of widespread brain abnormalities in patients' groups with higher percentage of male is not surprising in SZ literature. Similarly to Bora et al. (2011), our results reveal a GM negative relationship related to the L-IFG, R-Ins, and bilateral thalamus in samples with a higher percentage of male patients. Volumetric variations have been related to different GM decreases in male/female patients with SZ (Mendrek and Mancini-Marïe, 2016), which to some extent may reflect different gender health development (Lotze et al., 2019).

Groups with a high percentage of patients undergoing antipsychotic treatment have been associated with more severe GM loss in the L-MFG, R-STG, and R-Ins. At present, the association between the antipsychotic medication and regional anatomical changes in SZ remains inconsistent (Lawrie, 2018). Taken in this context, our results provide voxel-based

evidence of localized effects related to antipsychotic drug usage. Cautious interpretations are needed due to the lack of longitudinal approach and the unappreciated contribution of other variables such as the severity of symptoms, which could variously correlate with an antipsychotic treatment and its duration, dosage and typology, as well as a more or less marked GM alteration (Fusar-Poli et al., 2013; Vita et al., 2015).

Small sample size impacts on GM findings in a double cluster of alteration, corresponding to the R-STG and the L-ACC. This result is consistent with a number of studies highlighting the importance of sufficiently large sample sizes in neuroimaging investigations in order to enhance reproducibility and decrease between-study heterogeneity (Chen et al., 2018; Ingre, 2013; Lorca-Puls et al., 2018). Although the CBMA approach tends to mitigate these issues, our findings further highlight that it is advisable to increase the number of patients to provide more robust results.

The absence of significant linear effect on GM volumes with chlorpromazine equivalents could be explained by the heterogeneity of antipsychotic drugs and of the times of exposure to the drugs (Vita et al., 2015). A similar explanation concerns the absence of linear association between positive and negative symptoms and GM alterations. These two dimensions of symptoms were evaluated with the PANSS positive and negative subscales, that include many items poorly correlated with these two symptomatic constructs, therefore introducing "noise" in the data (Fountoulakis et al., 2019). More specific and targeted evaluations of signs and symptoms of SZ, possibly based on the factor analysis of the PANSS (Kay et al., 1987) and taking into account also disorganized, depressive and cognitive symptoms, should be recommended in all neuroimaging studies on SZ in order to better detect significant correlation between imaging and specific aspects of the disorder.

4.6. Innovation and strengths

Our work partially confirms the results of the previous CBMAs about SZ stages and provides new evidence for their better characterization. First, we were able to include the largest number of published experiments due to the rapid growth of the field. The balance between sensitivity and susceptibility to false positive effects was therefore maximized and the power of the meta-analysis increased (Müller et al., 2018).

Second, published articles that pooled together both patients with short and long duration of illness were excluded and studies about HR were included, allowing us to study morphological and functional patterns related to specific stages of the disorder, including the prodromal phase, so as to exclude possible confounding elements derived from other diagnosis belonging to the SSD. For the comparisons between clinical groups we added a set of conjunction and contrast analyses, allowing us to statistically derive common and potentially distinctive neuroanatomical markers.

Third, we employed a new revised version of the ALE method and implemented a conservative thresholding. To our knowledge, this is the first ALE study on SZ using both the corrected GingerALE version and cluster-level FWE correction, ensuring an adequate type I error control and the maximum statistical rigor (Eickhoff et al., 2017, 2016). Importantly, the involvement of ALE-derived brain regions was further demonstrated via voxel-wise permutation tests.

Fourth, we found the neuroanatomical effects of male sex, sample size, image smoothing level and medication. Although these results should be interpreted with caution, as meta-regression tested the mean-relation between samples (Radua et al., 2012) and a different algorithm than ALE was employed, they might shed light on the impact of certain variables on GM findings, as well as improve future sampling and methodological strategies.

Fifth, the quantitative functional characterization used in this study ensured a comprehensive and objective behavioral association to GM findings, and explored mental functions prominently linked to different stages of SZ. This choice was motivated by the long-standing debate concerning the limits of observer-dependent and region-to-behavior inference in the field of neuroimaging (Scarpazza and De Simone, 2016).

4.7. Limitations and challenges

The present study has general limitations inherent to meta-analytic approach. The ALE technique is based on stereotactic foci reported by published articles and, therefore, may be potentially affected by the publication bias against null results (i.e. file-drawer problem) (Müller et al., 2018). Other bias could relate to the selective local maxima evaluation, excluding the remaining significant voxels of variation. However, it should be noted this standardized procedure in the neuroimaging field and in CBMA, can decrease the probability of making spatial errors (Eickhoff et al., 2009; Radua et al., 2012). We also note that the incomplete reporting of included investigations data may hamper some meta-regression results. For instance, a number of studies do not provided information about medication dosage (49/90 studies, 54.5 % of the total) or PANSS positive and negative scores (34/90 studies, 37.7 % of the total).

Finally, it is important to point out that our approach cannot determine causality of illness progression due to the lack of longitudinal design. However, robust cross-sectional meta- and mega-analyses are also essential to further clarify this issue and build a more integrative view (Meisenzahl et al., 2008; Pantelis et al., 2005; Torres et al., 2016; Zhao et al., 2018). In this regard, our approach has been highly sensitive in quantifying more widespread structural changes in the chronic condition than in the first period after the onset of the disorder; in addition, it has been able to identify certain common alteration patterns that could represent critical starting points in the propagation of damage and clinical manifestations of the disease.

Although we have consolidated the existing literature by identifying the 'if' and 'where' of GM changes in SZ, future investigations are needed to detect 'how' these changes co-occur in a network-like architecture and diffuse at different stages of disease. Moreover, the development of novel 'reverse inference' methodologies is greatly needed in order to disentangle the pathological brain landscape, as well as to identify the cerebral regions exhibiting high alteration specificity for the SZ condition.

5. Conclusions

This meta-analysis provides a quantitative summary of voxel-based results on different stages of SZ published over the last two-decades. Our findings support the current framework that considers SZ as a neurodevelopmental disease with a neuroprogressive component, but also update and characterize the pathological landscape of SZ stages. The heterogeneity in the underlying literature notwithstanding, we have found high-quality evidence for convergent GM loss in cortico-striatal-limbic hub regions. It is worth noting that the GM reduction in the R-ACC is present both in the c-HR group and in SZ groups; if confirmed, this result would make the alteration of R-ACC a possible marker of disease progression. A widespread GM loss has been found in the RDSZ patients, mainly in frontal and temporal areas of the left cerebral hemisphere. A further spread of the GM reduction in homotopic areas of the right hemisphere as well as into subcortical region has been found in the ChSZ subjects. Albeit in cross-sectional and meta-analytic manner, these results are likely to reflect the temporal progression of SZ and the interhemispheric and subcortical diffusion of its neuroanatomical alteration. The development of novel neuroimaging methodologies and of longitudinal multicenter and multimodal studies is needed to advance in this field. We are therefore hopeful that the approach employed here may pave the way for research on possible diagnostic and neuroimaging biomarkers of SZ staging, as well as on the identification of new therapeutics target that could be addressed not only with psychopharmacological treatments but also with focused magnetic and/or non-invasive electric stimulation and with evidence-based psychosocial rehabilitation

programs.

Research data availability

Alteration maps are available upon reasonable request.

Funding

This study was supported by the Fondazione Carlo Molo (F Cauda, PI) and Ministero dell'Istruzione, dell'Università e della Ricerca - MIUR Projects "Dipartimenti di Eccellenza 2018−2022" to the Dept. of Neuroscience "Rita Levi Montalcini" (P Rocca, PI).

CRediT authorship contribution statement

Donato Liloia: Conceptualization, Methodology, Formal analysis, Investigation, Data curation, Writing - original draft, Visualization. **Claudio Brasso:** Methodology, Data curation, Writing - original draft. **Franco Cauda:** Writing - review & editing, Supervision, Project administration, Funding acquisition. **Lorenzo Mancuso:** Formal analysis, Writing - review & editing. **Andrea Nani:** Writing - review & editing. **Jordi Manuello:** Investigation. **Tommaso Costa:** Writing - review & editing, Formal analysis, Investigation, Supervision. **Sergio Duca:** Project administration. **Paola Rocca:** Writing - review & editing, Supervision, Project administration, Funding acquisition.

Declaration of Competing Interest

The authors report no declarations of interest.

Appendix A. Supplementary data

Supplementary material related to this article can be found, in the online version, at doi:https://doi.org/10.1016/j.neubiorev.2021.01.010.

References

Adriano, F., Spoletini, I., Caltagirone, C., Spalletta, G., 2010. Updated meta-analyses reveal thalamus volume reduction in patients with first-episode and chronic schizophrenia. Schizophr. Res. 123, 1–14. https://doi.org/10.1016/j.schres.2010.07.007.

Albajes-Eizagirre, A., Radua, J., 2018. What do results from coordinate-based meta-analyses tell us? NeuroImage 176, 550–553. https://doi.org/10.1016/j.neuroimage.2018.04.065.

Albajes-Eizagirre, A., Solanes, A., Vieta, E., Radua, J., 2019. Voxel-based meta-analysis via permutation of subject images (PSI): theory and implementation for SDM. NeuroImage 186, 174–184. https://doi.org/10.1016/j.neuroimage.2018.10.077.

Albrecht, F., Bisenius, S., Neumann, J., Whitwell, J., Schroeter, M.L., 2019. Atrophy in midbrain & cerebral/cerebellar pedunculi is characteristic for progressive supranuclear palsy - A double-validation whole-brain meta-analysis. Neuroimage Clin. 22, 101722 https://doi.org/10.1016/j.nicl.2019.101722.

Allen, P., Stephan, K.E., Mechelli, A., Day, F., Ward, N., Dalton, J., Williams, S.C., McGuire, P., 2010. Cingulate activity and fronto-temporal connectivity in people with prodromal signs of psychosis. NeuroImage 49, 947–955. https://doi.org/10.1016/j.neuroimage.2009.08.038.

Allman, J.M., Tetreault, N.A., Hakeem, A.Y., Manaye, K.F., Semendeferi, K., Erwin, J.M., Park, S., Goubert, V., Hof, P.R., 2010. The von Economo neurons in frontoinsular and anterior cingulate cortex in great apes and humans. Brain Struct. Funct. 214, 495–517. https://doi.org/10.1007/s00429-010-0254-0.

Allman, J.M., Tetreault, N.A., Hakeem, A.Y., Manaye, K.F., Semendeferi, K., Erwin, J.M., Park, S., Goubert, V., Hof, P.R., 2011. The von Economo neurons in the frontoinsular and anterior cingulate cortex. Ann. N. Y. Acad. Sci. 1225, 59–71. https://doi.org/10.1111/j.1749-6632.2011.06011.x.

Anderson, K.K., Voineskos, A., Mulsant, B.H., George, T.P., McKenzie, K.J., 2014. The role of untreated psychosis in neurodegeneration: a review of hypothesized mechanisms of neurotoxicity in first-episode psychosis. Canadian journal of psychiatry. Revue canadienne de psychiatrie 59, 513–517. https://doi.org/10.1177/070674371405901003.

Andreasen, N.C., 2010. The lifetime trajectory of schizophrenia and the concept of neurodevelopment. Dialogues Clin. Neurosci. 12, 409–415. https://doi.org/10.31887/DCNS.2010.12.3/nandreasen.

Andreou, C., Borgwardt, S., 2020. Structural and functional imaging markers for susceptibility to psychosis. Mol. Psychiatry. https://doi.org/10.1038/s41380-020-0679-7.

Asami, T., Bouix, S., Whitford, T.J., Shenton, M.E., Salisbury, D.F., McCarley, R.W., 2012. Longitudinal loss of gray matter volume in patients with first-episode schizophrenia: DARTEL automated analysis and ROI validation. NeuroImage 59, 986–996. https://doi.org/10.1016/j.neuroimage.2011.08.066.

Ashburner, J., Friston, K.J., 2000. Voxel-based morphometry—the methods. NeuroImage 11, 805–821. https://doi.org/10.1006/nimg.2000.0582.

Ashe, P.C., Berry, M.D., Boulton, A.A., 2001. Schizophrenia, a neurodegenerative disorder with neurodevelopmental antecedents. Prog. Neuropsychopharmacol. Biol. Psychiatry 25, 691–707. https://doi.org/10.1016/s0278-5846(01)00159-2.

Avram, M., Brandl, F., Bäuml, J., Sorg, C., 2018. Cortico-thalamic hypo- and hyperconnectivity extend consistently to basal ganglia in schizophrenia. Neuropsychopharmacology 43, 2239–2248. https://doi.org/10.1038/s41386-018-0059-z.

Belyk, M., Brown, S., Lim, J., Kotz, S.A., 2017. Convergence of semantics and emotional expression within the IFG pars orbitalis. NeuroImage 156, 240–248. https://doi.org/10.1016/j.neuroimage.2017.04.020.

Bennett, C.M., Wolford, G.L., Miller, M.B., 2009. The principled control of false positives in neuroimaging. Soc. Cogn. Affect. Neurosci. 4, 417–422. https://doi.org/10.1093/scan/nsp053.

Bernard, J.A., Goen, J.R.M., Maldonado, T., 2017. A case for motor network contributions to schizophrenia symptoms: evidence from resting-state connectivity. Hum. Brain Mapp. 38, 4535–4545. https://doi.org/10.1002/hbm.23680.

Birur, B., Kraguljac, N.V., Shelton, R.C., Lahti, A.C., 2017. Brain structure, function, and neurochemistry in schizophrenia and bipolar disorder-a systematic review of the magnetic resonance neuroimaging literature. NPJ Schizophr. 3, 15. https://doi.org/10.1038/s41537-017-0013-9.

Biswal, B.B., Mennes, M., Zuo, X.N., Gohel, S., Kelly, C., Smith, S.M., Beckmann, C.F., Adelstein, J.S., Buckner, R.L., Colcombe, S., Dogonowski, A.M., Ernst, M., Fair, D., Hampson, M., Hoptman, M.J., Hyde, J.S., Kiviniemi, V.J., Kotter, R., Li, S.J., Lin, C. P., Lowe, M.J., Mackay, C., Madden, D.J., Madsen, K.H., Margulies, D.S., Mayberg, H.S., McMahon, K., Monk, C.S., Mostofsky, S.H., Nagel, B.J., Pekar, J.J., Peltier, S.J., Petersen, S.E., Riedl, V., Rombouts, S.A., Rypma, B., Schlaggar, B.L., Schmidt, S., Seidler, R.D., Siegle, G.J., Sorg, C., Teng, G.J., Veijola, J., Villringer, A., Walter, M., Wang, L., Weng, X.C., Whitfield-Gabrieli, S., Williamson, P., Windischberger, C., Zang, Y.F., Zhang, H.Y., Castellanos, F.X., Milham, M.P., 2010. Toward discovery science of human brain function. Proc. Natl. Acad. Sci. U.S.A. 107, 4734–4739. https://doi.org/10.1073/pnas.0911855107.

Bonner-Jackson, A., Haut, K., Csernansky, J.G., Barch, D.M., 2005. The influence of encoding strategy on episodic memory and cortical activity in schizophrenia. Biol. Psychiatry 58, 47–55. https://doi.org/10.1016/j.biopsych.2005.05.011.

Boos, H.B., Aleman, A., Cahn, W., Hulshoff Pol, H., Kahn, R.S., 2007. Brain volumes in relatives of patients with schizophrenia: a meta-analysis. Arch. Gen. Psychiatry 64, 297–304. https://doi.org/10.1001/archpsyc.64.3.297.

Bora, E., Fornito, A., Radua, J., Walterfang, M., Seal, M., Wood, S.J., Yucel, M., Velakoulis, D., Pantelis, C., 2011. Neuroanatomical abnormalities in schizophrenia: a multimodal voxelwise meta-analysis and meta-regression analysis. Schizophr. Res. 127, 46–57. https://doi.org/10.1016/j.schres.2010.12.020.

Bora, E., Fornito, A., Yucel, M., Pantelis, C., 2012. The effects of gender on grey matter abnormalities in major psychoses: a comparative voxelwise meta-analysis of schizophrenia and bipolar disorder. Psychol. Med. 42, 295–307. https://doi.org/10.1017/s0033291711001450.

Bora, E., Akdede, B.B., Alptekin, K., 2017. The relationship between cognitive impairment in schizophrenia and metabolic syndrome: a systematic review and meta-analysis. Psychol. Med. 47, 1030–1040. https://doi.org/10.1017/s0033291716003366.

Brickman, A.M., Buchsbaum, M.S., Shihabuddin, L., Byne, W., Newmark, R.E., Brand, J., Ahmed, S., Mitelman, S.A., Hazlett, E.A., 2004. Thalamus size and outcome in schizophrenia. Schizophr. Res. 71, 473–484. https://doi.org/10.1016/j.schres.2004.03.011.

Brüne, M., Schöbel, A., Karau, R., Benali, A., Faustmann, P.M., Juckel, G., Petrasch-Parwez, E., 2010. Von Economo neuron density in the anterior cingulate cortex is reduced in early onset schizophrenia. Acta Neuropathol. 119, 771–778. https://doi.org/10.1007/s00401-010-0673-2.

Brüne, M., Schöbel, A., Karau, R., Faustmann, P.M., Dermietzel, R., Juckel, G., Petrasch-Parwez, E., 2011. Neuroanatomical correlates of suicide in psychosis: the possible role of von Economo neurons. PLoS One 6, e20936. https://doi.org/10.1371/journal.pone.0020936.

Buoli, M., Serati, M., Caldiroli, A., Cremaschi, L., Altamura, A.C., 2017. Neurodevelopmental versus neurodegenerative model of schizophrenia and bipolar disorder: comparison with physiological brain development and aging. Psychiatr. Danub. 29, 24–27. https://doi.org/10.24869/psyd.2017.24.

Butti, C., Santos, M., Uppal, N., Hof, P.R., 2013. Von Economo neurons: clinical and evolutionary perspectives. Cortex 49, 312–326. https://doi.org/10.1016/j.cortex.2011.10.004.

Byne, W., Buchsbaum, M.S., Kemether, E., Hazlett, E.A., Shinwari, A., Mitropoulou, V., Siever, L.J., 2001. Magnetic resonance imaging of the thalamic mediodorsal nucleus and pulvinar in schizophrenia and schizotypal personality disorder. Arch. Gen. Psychiatry 58, 133–140. https://doi.org/10.1001/archpsyc.58.2.133.

Byne, W., Hazlett, E.A., Buchsbaum, M.S., Kemether, E., 2009. The thalamus and schizophrenia: current status of research. Acta Neuropathol. 117, 347–368. https://doi.org/10.1007/s00401-008-0404-0.

Cannon, T.D., Sun, F., McEwen, S.J., Papademetris, X., He, G., van Erp, T.G., Jacobson, A., Bearden, C.E., Walker, E., Hu, X., Zhou, L., Seidman, L.J.,

Thermenos, H.W., Cornblatt, B., Olvet, D.M., Perkins, D., Belger, A., Cadenhead, K., Tsuang, M., Mirzakhanian, H., Addington, J., Frayne, R., Woods, S.W., McGlashan, T.H., Constable, R.T., Qiu, M., Mathalon, D.H., Thompson, P., Toga, A. W., 2014. Reliability of neuroanatomical measurements in a multisite longitudinal study of youth at risk for psychosis. Hum. Brain Mapp. 35, 2424–2434. https://doi.org/10.1002/hbm.22338.

Canu, E., Agosta, F., Filippi, M., 2015. A selective review of structural connectivity abnormalities of schizophrenic patients at different stages of the disease. Schizophr. Res. 161, 19–28. https://doi.org/10.1016/j.schres.2014.05.020.

Cauda, F., Geminiani, G.C., Vercelli, A., 2014. Evolutionary appearance of von Economo's neurons in the mammalian cerebral cortex. Front. Hum. Neurosci. 8, 104. https://doi.org/10.3389/fnhum.2014.00104.

Cauda, F., Nani, A., Costa, T., Palermo, S., Tatu, K., Manuello, J., Duca, S., Fox, P.T., Keller, R., 2018. The morphometric co-atrophy networking of schizophrenia, autistic and obsessive spectrum disorders. Hum. Brain Mapp. https://doi.org/10.1002/hbm.23952.

Cauda, F., Nani, A., Manuello, J., Liloia, D., Tatu, K., Vercelli, U., Duca, S., Fox, P.T., Costa, T., 2019. The alteration landscape of the cerebral cortex. NeuroImage 184, 359–371. https://doi.org/10.1016/j.neuroimage.2018.09.036.

Chan, R.C., Di, X., McAlonan, G.M., Gong, Q.Y., 2011. Brain anatomical abnormalities in high-risk individuals, first-episode, and chronic schizophrenia: an activation likelihood estimation meta-analysis of illness progression. Schizophr. Bull. 37, 177–188. https://doi.org/10.1093/schbul/sbp073.

Charlson, F.J., Ferrari, A.J., Santomauro, D.F., Diminic, S., Stockings, E., Scott, J.G., McGrath, J.J., Whiteford, H.A., 2018. Global epidemiology and burden of schizophrenia: findings from the global burden of disease study 2016. Schizophr. Bull. 44, 1195–1203. https://doi.org/10.1093/schbul/sby058.

Chen, Z., Deng, W., Gong, Q., Huang, C., Jiang, L., Li, M., He, Z., Wang, Q., Ma, X., Wang, Y., Chua, S.E., McAlonan, G.M., Sham, P.C., Collier, D.A., McGuire, P., Li, T., 2014. Extensive brain structural network abnormality in first-episode treatment-naive patients with schizophrenia: morphometrical and covariation study. Psychol. Med. 44, 2489–2501. https://doi.org/10.1017/s003329171300319x.

Chen, X., Lu, B., Yan, C.G., 2018. Reproducibility of R-fMRI metrics on the impact of different strategies for multiple comparison correction and sample sizes. Hum. Brain Mapp. 39, 300–318. https://doi.org/10.1002/hbm.23843.

Collin, G., Seidman, L.J., Keshavan, M.S., Stone, W.S., Qi, Z., Zhang, T., Tang, Y., Li, H., Anteraper, S.A., Niznikiewicz, M.A., McCarley, R.W., Shenton, M.E., Wang, J., Whitfield-Gabrieli, S., 2018. Functional connectome organization predicts conversion to psychosis in clinical high-risk youth from the SHARP program. Mol. Psychiatry. https://doi.org/10.1038/s41380-018-0288-x.

Compton, M.T., Lunden, A., Cleary, S.D., Pauselli, L., Alolayan, Y., Halpern, B., Broussard, B., Crisafio, A., Capulong, L., Balducci, P.M., Bernardini, F., Covington, M.A., 2018. The aprosody of schizophrenia: computationally derived acoustic phonetic underpinnings of monotone speech. Schizophr. Res. 197, 392–399. https://doi.org/10.1016/j.schres.2018.01.007.

Cooper, D., Barker, V., Radua, J., Fusar-Poli, P., Lawrie, S.M., 2014. Multimodal voxel-based meta-analysis of structural and functional magnetic resonance imaging studies in those at elevated genetic risk of developing schizophrenia. Psychiatry Res. 221, 69–77. https://doi.org/10.1016/j.pscychresns.2013.07.008.

Corbetta, M., Kincade, J.M., Shulman, G.L., 2002. Neural systems for visual orienting and their relationships to spatial working memory. J. Cogn. Neurosci. 14, 508–523. https://doi.org/10.1162/089892902317362029.

Crossley, N.A., Mechelli, A., Scott, J., Carletti, F., Fox, P.T., McGuire, P., Bullmore, E.T., 2014. The hubs of the human connectome are generally implicated in the anatomy of brain disorders. Brain 137, 2382–2395. https://doi.org/10.1093/brain/awu132.

Davidson, L.L., Heinrichs, R.W., 2003. Quantification of frontal and temporal lobe brain-imaging findings in schizophrenia: a meta-analysis. Psychiatry Res. 122, 69–87. https://doi.org/10.1016/s0925-4927(02)00118-x.

Davis, J., Moylan, S., Harvey, B.H., Maes, M., Berk, M., 2014. Neuroprogression in schizophrenia: pathways underpinning clinical staging and therapeutic corollaries. Aust. N. Z. J. Psychiatry 48, 512–529. https://doi.org/10.1177/0004867414533012.

Dembler-Stamm, T., Fiebig, J., Heinz, A., Gallinat, J., 2018. Sexual dysfunction in unmedicated patients with schizophrenia and in healthy controls. Pharmacopsychiatry 51, 251–256. https://doi.org/10.1055/s-0044-100627.

Eickhoff, S.B., Laird, A.R., Grefkes, C., Wang, L.E., Zilles, K., Fox, P.T., 2009. Coordinate-based activation likelihood estimation meta-analysis of neuroimaging data: a random-effects approach based on empirical estimates of spatial uncertainty. Hum. Brain Mapp. 30, 2907–2926. https://doi.org/10.1002/hbm.20718.

Eickhoff, S.B., Bzdok, D., Laird, A.R., Roski, C., Caspers, S., Zilles, K., Fox, P.T., 2011. Co-activation patterns distinguish cortical modules, their connectivity and functional differentiation. NeuroImage 57, 938–949. https://doi.org/10.1016/j.neuroimage.2011.05.021.

Eickhoff, S.B., Bzdok, D., Laird, A.R., Kurth, F., Fox, P.T., 2012. Activation likelihood estimation meta-analysis revisited. NeuroImage 59, 2349–2361. https://doi.org/10.1016/j.neuroimage.2011.09.017.

Eickhoff, S.B., Nichols, T.E., Laird, A.R., Hoffstaedter, F., Amunts, K., Fox, P.T., Bzdok, D., Eickhoff, C.R., 2016. Behavior, sensitivity, and power of activation likelihood estimation characterized by massive empirical simulation. NeuroImage 137, 70–85. https://doi.org/10.1016/j.neuroimage.2016.04.072.

Eickhoff, S.B., Laird, A.R., Fox, P.M., Lancaster, J.L., Fox, P.T., 2017. Implementation errors in the GingerALE software: description and recommendations. Hum. Brain Mapp. 38, 7–11. https://doi.org/10.1002/hbm.23342.

Ellison-Wright, I., Bullmore, E., 2010. Anatomy of bipolar disorder and schizophrenia: a meta-analysis. Schizophr. Res. 117, 1–12. https://doi.org/10.1016/j.schres.2009.12.022.

Ellison-Wright, I., Glahn, D.C., Laird, A.R., Thelen, S.M., Bullmore, E., 2008. The anatomy of first-episode and chronic schizophrenia: an anatomical likelihood estimation meta-analysis. Am. J. Psychiatry 165, 1015–1023. https://doi.org/10.1176/appi.ajp.2008.07101562.

Enge, A., Friederici, A.D., Skeide, M.A., 2020. A meta-analysis of fMRI studies of language comprehension in children. NeuroImage 215, 116858. https://doi.org/10.1016/j.neuroimage.2020.116858.

Falkenberg, I., Valmaggia, L., Byrnes, M., Frascarelli, M., Jones, C., Rocchetti, M., Straube, B., Badger, S., McGuire, P., Fusar-Poli, P., 2015. Why are help-seeking subjects at ultra-high risk for psychosis help-seeking? Psychiatry Res. 228, 808–815. https://doi.org/10.1016/j.psychres.2015.05.018.

Ferri, F., Salone, A., Ebisch, S.J., De Berardis, D., Romani, G.L., Ferro, F.M., Gallese, V., 2012. Action verb understanding in first-episode schizophrenia: is there evidence for a simulation deficit? Neuropsychologia 50, 988–996. https://doi.org/10.1016/j.neuropsychologia.2012.02.005.

Ferri, J., Ford, J.M., Roach, B.J., Turner, J.A., van Erp, T.G., Voyvodic, J., Preda, A., Belger, A., Bustillo, J., O'Leary, D., Mueller, B.A., Lim, K.O., McEwen, S.C., Calhoun, V.D., Diaz, M., Glover, G., Greve, D., Wible, C.G., Vaidya, J.G., Potkin, S.G., Mathalon, D.H., 2018. Resting-state thalamic dysconnectivity in schizophrenia and relationships with symptoms. Psychol. Med. 48, 2492–2499. https://doi.org/10.1017/s003329171800003x.

Fervaha, G., Remington, G., 2013. Neuroimaging findings in schizotypal personality disorder: a systematic review. Prog. Neuropsychopharmacol. Biol. Psychiatry 43, 96–107. https://doi.org/10.1016/j.pnpbp.2012.11.014.

Fornara, G.A., Papagno, C., Berlingeri, M., 2017. A neuroanatomical account of mental time travelling in schizophrenia: a meta-analysis of functional and structural neuroimaging data. Neurosci. Biobehav. Rev. 80, 211–222. https://doi.org/10.1016/j.neubiorev.2017.05.027.

Fornito, A., Yung, A.R., Wood, S.J., Phillips, L.J., Nelson, B., Cotton, S., Velakoulis, D., McGorry, P.D., Pantelis, C., Yucel, M., 2008. Anatomic abnormalities of the anterior cingulate cortex before psychosis onset: an MRI study of ultra-high-risk individuals. Biol. Psychiatry 64, 758–765. https://doi.org/10.1016/j.biopsych.2008.05.032.

Fornito, A., Yucel, M., Patti, J., Wood, S.J., Pantelis, C., 2009. Mapping grey matter reductions in schizophrenia: an anatomical likelihood estimation analysis of voxel-based morphometry studies. Schizophr. Res. 108, 104–113. https://doi.org/10.1016/j.schres.2008.12.011.

Fountoulakis, K.N., Dragioti, E., Theofilidis, A.T., Wikilund, T., Atmatzidis, X., Nimatoudis, I., Thys, E., Wampers, M., Hranov, L., Hristova, T., Aptalidis, D., Milev, R., Iftene, F., Spaniel, F., Knytl, P., Furstova, P., From, T., Karlsson, H., Walta, M., Salokangas, R.K.R., Azorin, J.M., Bouniard, J., Montant, J., Juckel, G., Haussleiter, I.S., Douzenis, A., Michopoulos, I., Ferentinos, P., Smyrnis, N., Mantonakis, L., Nemes, Z., Gonda, X., Vajda, D., Juhasz, A., Shrivastava, A., Waddington, J., Pompili, M., Comparelli, A., Corigliano, V., Rancans, E., Navickas, A., Hilbig, J., Bukelskis, L., Injac Stevovic, L., Vodopic, S., Esan, O., Oladele, O., Osunbote, C., Rybakowski, J., Wojciak, P., Domowicz, K., Figueira, M.L., Linhares, L., Crawford, J., Panfil, A.L., Smirnova, D., Izmailova, O., Lecic-Tosevski, D., Temmingh, H., Howells, F., Bobes, J., Garcia-Portilla, M.P., Garcia-Alvarez, L., Erzin, G., Karadag, H., De Sousa, A., Bendre, A., Hoschl, C., Bredicean, C., Papava, I., Vukovic, O., Pejuskovic, B., Russell, V., Athanasiadis, L., Konsta, A., Stein, D., Berk, M., Dean, O., Tandon, R., Kasper, S., De Hert, M., 2019. Staging of schizophrenia with the use of PANSS: an international multi-center study. Int. J. Neuropsychopharmacol. 22, 681–697. https://doi.org/10.1093/ijnp/pyz053.

Fountoulakis, K.N., Dragioti, E., Theofilidis, A.T., Wiklund, T., Atmatzidis, X., Nimatoudis, I., Thys, E., Wampers, M., Hranov, L., Hristova, T., Aptalidis, D., Milev, R., Iftene, F., Spaniel, F., Knytl, P., Furstova, P., From, T., Karlsson, H., Walta, M., Salokangas, R.K.R., Azorin, J.M., Bouniard, J., Montant, J., Juckel, G., Haussleiter, I.S., Douzenis, A., Michopoulos, I., Ferentinos, P., Smyrnis, N., Mantonakis, L., Nemes, Z., Gonda, X., Vajda, D., Juhasz, A., Shrivastava, A., Waddington, J., Pompili, M., Comparelli, A., Corigliano, V., Rancans, E., Navickas, A., Hilbig, J., Bukelskis, L., Stevovic, L.I., Vodopic, S., Esan, O., Oladele, O., Osunbote, C., Rybakowski, J., Wojciak, P., Domowicz, K., Figueira, M.L., Linhares, L., Crawford, J., Panfil, A.L., Smirnova, D., Izmailova, O., Lecic-Tosevski, D., Temmingh, H., Howells, F., Bobes, J., Garcia-Portilla, M.P., Garcia-Alvarez, L., Erzin, G., Karadag, H., De Sousa, A., Bendre, A., Hoschl, C., Bredicean, C., Papava, I., Vukovic, O., Pejuskovic, B., Russell, V., Athanasiadis, L., Konsta, A., Stein, D., Berk, M., Dean, O., Tandon, R., Kasper, S., De Hert, M., 2020. Modeling psychological function in patients with schizophrenia with the PANSS: an international multi-center study. CNS Spectr. 1–9. https://doi.org/10.1017/s1092852920001091.

Fox, P.T., Lancaster, J.L., Laird, A.R., Eickhoff, S.B., 2014. Meta-analysis in human neuroimaging: computational modeling of large-scale databases. Annu. Rev. Neurosci. 37, 409–434. https://doi.org/10.1146/annurev-neuro-062012-170320.

Fusar-Poli, P., Borgwardt, S., Crescini, A., Deste, G., Kempton, M.J., Lawrie, S., Mc Guire, P., Sacchetti, E., 2011a. Neuroanatomy of vulnerability to psychosis: a voxel-based meta-analysis. Neurosci. Biobehav. Rev. 35, 1175–1185. https://doi.org/10.1016/j.neubiorev.2010.12.005.

Fusar-Poli, P., Broome, M.R., Woolley, J.B., Johns, L.C., Tabraham, P., Bramon, E., Valmaggia, L., Williams, S.C., McGuire, P., 2011b. Altered brain function directly related to structural abnormalities in people at ultra high risk of psychosis: longitudinal VBM-fMRI study. J. Psychiatr. Res. 45, 190–198. https://doi.org/10.1016/j.jpsychires.2010.05.012.

Fusar-Poli, P., Bonoldi, I., Yung, A.R., Borgwardt, S., Kempton, M.J., Valmaggia, L., Barale, F., Caverzasi, E., McGuire, P., 2012. Predicting psychosis: meta-analysis of transition outcomes in individuals at high clinical risk. Arch. Gen. Psychiatry 69, 220–229. https://doi.org/10.1001/archgenpsychiatry.2011.1472.

Fusar-Poli, P., Smieskova, R., Kempton, M.J., Ho, B.C., Andreasen, N.C., Borgwardt, S., 2013. Progressive brain changes in schizophrenia related to antipsychotic treatment? A meta-analysis of longitudinal MRI studies. Neurosci. Biobehav. Rev. 37, 1680–1691. https://doi.org/10.1016/j.neubiorev.2013.06.001.

Fusar-Poli, P., Smieskova, R., Serafini, G., Politi, P., Borgwardt, S., 2014. Neuroanatomical markers of genetic liability to psychosis and first episode psychosis: a voxelwise meta-analytical comparison. World J. Biol. Psychiatry 15, 219–228. https://doi.org/10.3109/15622975.2011.630408.

Glahn, D.C., Laird, A.R., Ellison-Wright, I., Thelen, S.M., Robinson, J.L., Lancaster, J.L., Bullmore, E., Fox, P.T., 2008. Meta-analysis of gray matter anomalies in schizophrenia: application of anatomic likelihood estimation and network analysis. Biol. Psychiatry 64, 774–781. https://doi.org/10.1016/j.biopsych.2008.03.031.

Glenthoj, L.B., Kristensen, T.D., Wenneberg, C., Hjorthoj, C., Nordentoft, M., 2020. Experiential negative symptoms are more predictive of real-life functional outcome than expressive negative symptoms in clinical high-risk states. Schizophr. Res. https://doi.org/10.1016/j.schres.2020.01.012.

Green, M.F., Horan, W.P., Lee, J., 2019. Nonsocial and social cognition in schizophrenia: current evidence and future directions. World Psychiatry 18, 146–161. https://doi.org/10.1002/wps.20624.

Hager, B.M., Keshavan, M.S., 2015. Neuroimaging biomarkers for psychosis. Curr. Behav. Neurosci. Rep. 2015, 1–10. https://doi.org/10.1007/s40473-015-0035-4.

Hoptman, M.J., Zuo, X.N., D'Angelo, D., Mauro, C.J., Butler, P.D., Milham, M.P., Javitt, D.C., 2012. Decreased interhemispheric coordination in schizophrenia: a resting state fMRI study. Schizophr. Res. 141, 1–7. https://doi.org/10.1016/j.schres.2012.07.027.

Horga, G., Bernacer, J., Dusi, N., Entis, J., Chu, K., Hazlett, E.A., Haznedar, M.M., Kemether, E., Byne, W., Buchsbaum, M.S., 2011. Correlations between ventricular enlargement and gray and white matter volumes of cortex, thalamus, striatum, and internal capsule in schizophrenia. Eur. Arch. Psychiatry Clin. Neurosci. 261, 467–476. https://doi.org/10.1007/s00406-011-0202-x.

Howard, J.D., Reynolds, R., Smith, D.E., Voss, J.L., Schoenbaum, G., Kahnt, T., 2020. Targeted stimulation of human orbitofrontal networks disrupts outcome-guided behavior. Curr. Biol. 30, 490–498. https://doi.org/10.1016/j.cub.2019.12.007 e494.

Hua, J., Blair, N.I.S., Paez, A., Choe, A., Barber, A.D., Brandt, A., Lim, I.A.L., Xu, F., Kamath, V., Pekar, J.J., van Zijl, P.C.M., Ross, C.A., Margolis, R.L., 2019. Altered functional connectivity between sub-regions in the thalamus and cortex in schizophrenia patients measured by resting state BOLD fMRI at 7T. Schizophr. Res. 206, 370–377. https://doi.org/10.1016/j.schres.2018.10.016.

Hummer, T.A., Yung, M.G., Goñi, J., Conroy, S.K., Francis, M.M., Mehdiyoun, N.F., Breier, A., 2020. Functional network connectivity in early-stage schizophrenia. Schizophr. Res. https://doi.org/10.1016/j.schres.2020.01.023.

Ingre, M., 2013. Why small low-powered studies are worse than large high-powered studies and how to protect against "trivial" findings in research: comment on Friston (2012). NeuroImage 81, 496–498. https://doi.org/10.1016/j.neuroimage.2013.03.030.

Isobe, M., Miyata, J., Hazama, M., Fukuyama, H., Murai, T., Takahashi, H., 2016. Multimodal neuroimaging as a window into the pathological physiology of schizophrenia: current trends and issues. Neurosci. Res. 102, 29–38. https://doi.org/10.1016/j.neures.2015.07.009.

Jaeger, J., 2018. Digit symbol substitution test: the case for sensitivity over specificity in neuropsychological testing. J. Clin. Psychopharmacol. 38, 513–519. https://doi.org/10.1097/JCP.0000000000000941.

Jeong, B., Wible, C.G., Hashimoto, R., Kubicki, M., 2009. Functional and anatomical connectivity abnormalities in left inferior frontal gyrus in schizophrenia. Hum. Brain Mapp. 30, 4138–4151. https://doi.org/10.1002/hbm.20835.

Jessen, F., Scherk, H., Traber, F., Theyson, S., Berning, J., Tepest, R., Falkai, P., Schild, H. H., Maier, W., Wagner, M., Block, W., 2006. Proton magnetic resonance spectroscopy in subjects at risk for schizophrenia. Schizophr. Res. 87, 81–88. https://doi.org/10.1016/j.schres.2006.06.011.

John, J.P., Lukose, A., Bagepally, B.S., Halahalli, H.N., Moily, N.S., Vijayakumari, A.A., Jain, S., 2015. A systematic examination of brain volumetric abnormalities in recent-onset schizophrenia using voxel-based, surface-based and region-of-interest-based morphometric analyses. J. Negat. Results Biomed. 14, 11. https://doi.org/10.1186/s12952-015-0030-z.

Jovicich, J., Czanner, S., Han, X., Salat, D., van der Kouwe, A., Quinn, B., Pacheco, J., Albert, M., Killiany, R., Blacker, D., Maguire, P., Rosas, D., Makris, N., Gollub, R., Dale, A., Dickerson, B.C., Fischl, B., 2009. MRI-derived measurements of human subcortical, ventricular and intracranial brain volumes: reliability effects of scan sessions, acquisition sequences, data analyses, scanner upgrade, scanner vendors and field strengths. NeuroImage 46, 177–192. https://doi.org/10.1016/j.neuroimage.2009.02.010.

Kahn, R.S., Keefe, R.S., 2013. Schizophrenia is a cognitive illness: time for a change in focus. JAMA Psychiatry 70, 1107–1112. https://doi.org/10.1001/jamapsychiatry.2013.155.

Kakeda, S., Korogi, Y., 2010. The efficacy of a voxel-based morphometry on the analysis of imaging in schizophrenia, temporal lobe epilepsy, and Alzheimer's disease/mild cognitive impairment: a review. Neuroradiology 52, 711–721. https://doi.org/10.1007/s00234-010-0717-2.

Kambeitz, J., Kambeitz-Ilankovic, L., Leucht, S., Wood, S., Davatzikos, C., Malchow, B., Falkai, P., Koutsouleris, N., 2015. Detecting neuroimaging biomarkers for schizophrenia: a meta-analysis of multivariate pattern recognition studies. Neuropsychopharmacology 40, 1742–1751. https://doi.org/10.1038/npp.2015.22.

Kay, S.R., Fiszbein, A., Opler, L.A., 1987. The positive and negative syndrome scale (PANSS) for schizophrenia. Schizophr. Bull. 13, 261–276. https://doi.org/10.1093/schbul/13.2.261.

Kebets, V., Holmes, A.J., Orban, C., Tang, S., Li, J., Sun, N., Kong, R., Poldrack, R.A., Yeo, B.T.T., 2019. Somatosensory-motor dysconnectivity spans multiple transdiagnostic dimensions of psychopathology. Biol. Psychiatry 86, 779–791. https://doi.org/10.1016/j.biopsych.2019.06.013.

Kemether, E.M., Buchsbaum, M.S., Byne, W., Hazlett, E.A., Haznedar, M., Brickman, A. M., Platholi, J., Bloom, R., 2003. Magnetic resonance imaging of mediodorsal, pulvinar, and centromedian nuclei of the thalamus in patients with schizophrenia. Arch. Gen. Psychiatry 60, 983–991. https://doi.org/10.1001/archpsyc.60.9.983.

Keshavan, M.S., 1999. Development, disease and degeneration in schizophrenia: a unitary pathophysiological model. J. Psychiatr. Res. 33, 513–521. https://doi.org/10.1016/s0022-3956(99)00033-3.

Keysers, C., Kaas, J.H., Gazzola, V., 2010. Somatosensation in social perception. Nature reviews. Neuroscience 11, 417–428. https://doi.org/10.1038/nrn2833.

Killgore, W.D., Rosso, I.M., Gruber, S.A., Yurgelun-Todd, D.A., 2009. Amygdala volume and verbal memory performance in schizophrenia and bipolar disorder. Cogn. Behav. Neurol. 22, 28–37. https://doi.org/10.1097/WNN.0b013e318192cc67.

Kindler, J., Michel, C., Schultze-Lutter, F., Felber, G., Hauf, M., Schimmelmann, B.G., Kaess, M., Hubl, D., Walther, S., 2019. Functional and structural correlates of abnormal involuntary movements in psychosis risk and first episode psychosis. Schizophr. Res. 212, 196–203. https://doi.org/10.1016/j.schres.2019.07.032.

Kochunov, P., Thompson, P.M., Hong, L.E., 2019. Toward high reproducibility and accountable heterogeneity in schizophrenia research. JAMA Psychiatry 76, 680–681. https://doi.org/10.1001/jamapsychiatry.2019.0208.

Koenders, L., Machielsen, M.W., van der Meer, F.J., van Gasselt, A.C., Meijer, C.J., van den Brink, W., Koeter, M.W., Caan, M.W., Cousijn, J., den Braber, A., van' t Ent, D., Rive, M.M., Schene, A.H., van de Giessen, E., Huyser, C., de Kwaasteniet, B.P., Veltman, D.J., de Haan, L., 2015. Brain volume in male patients with recent onset schizophrenia with and without cannabis use disorders. J. Psychiatry Neurosci. 40, 197–206. https://doi.org/10.1503/jpn.140081.

Koutsouleris, N., Davatzikos, C., Borgwardt, S., Gaser, C., Bottlender, R., Frodl, T., Falkai, P., Riecher-Rossler, A., Moller, H.J., Reiser, M., Pantelis, C., Meisenzahl, E., 2014. Accelerated brain aging in schizophrenia and beyond: a neuroanatomical marker of psychiatric disorders. Schizophr. Bull. 40, 1140–1153. https://doi.org/10.1093/schbul/sbt142.

Krause, M., Theiss, C., Brüne, M., 2017. Ultrastructural alterations of von economo neurons in the anterior cingulate cortex in schizophrenia. Anat. Rec. (Hoboken, N.J. : 2007) 300, 2017–2024. https://doi.org/10.1002/ar.23635.

Lancaster, J.L., Tordesillas-Gutierrez, D., Martinez, M., Salinas, F., Evans, A., Zilles, K., Mazziotta, J.C., Fox, P.T., 2007. Bias between MNI and Talairach coordinates analyzed using the ICBM-152 brain template. Hum. Brain Mapp. 28, 1194–1205. https://doi.org/10.1002/hbm.20345.

Lancaster, J.L., Laird, A.R., Eickhoff, S.B., Martinez, M.J., Fox, P.M., Fox, P.T., 2012. Automated regional behavioral analysis for human brain images. Front. Neuroinform. 6, 23. https://doi.org/10.3389/fninf.2012.00023.

Lawrie, S.M., 2018. Are structural brain changes in schizophrenia related to antipsychotic medication? A narrative review of the evidence from a clinical perspective. Ther. Adv. Psychopharmacol. 8, 319–326. https://doi.org/10.1177/2045125318782306.

Lee, J.S., Jung, S., Park, I.H., Kim, J.J., 2015. Neural basis of Anhedonia and amotivation in patients with schizophrenia: the role of reward system. Curr. Neuropharmacol. 13, 750–759. https://doi.org/10.2174/1570159x13666150612230333.

Li, T., Wang, Q., Zhang, J., Rolls, E.T., Yang, W., Palaniyappan, L., Zhang, L., Cheng, W., Yao, Y., Liu, Z., Gong, X., Luo, Q., Tang, Y., Crow, T.J., Broome, M.R., Xu, K., Li, C., Wang, J., Liu, Z., Lu, G., Wang, F., Feng, J., 2017. Brain-wide analysis of functional connectivity in first-episode and chronic stages of schizophrenia. Schizophr. Bull. 43, 436–448. https://doi.org/10.1093/schbul/sbw099.

Li, Y., Li, W.X., Xie, D.J., Wang, Y., Cheung, E.F.C., Chan, R.C.K., 2018. Grey matter reduction in the caudate nucleus in patients with persistent negative symptoms: an ALE meta-analysis. Schizophr. Res. 192, 9–15. https://doi.org/10.1016/j.schres.2017.04.005.

Li, C., Liu, W., Guo, F., Wang, X., Kang, X., Xu, Y., Xi, Y., Wang, H., Zhu, Y., Yin, H., 2019a. Voxel-based morphometry results in first-episode schizophrenia: a comparison of publicly available software packages. Brain Imaging Behav. https://doi.org/10.1007/s11682-019-00172-x.

Li, M., Li, X., Das, T.K., Deng, W., Li, Y., Zhao, L., Ma, X., Wang, Y., Yu, H., Meng, Y., Wang, Q., Palaniyappan, L., Li, T., 2019b. Prognostic utility of multivariate morphometry in schizophrenia. Front. Psychiatry 10, 245. https://doi.org/10.3389/fpsyt.2019.00245.

Li, S., Hu, N., Zhang, W., Tao, B., Dai, J., Gong, Y., Tan, Y., Cai, D., Lui, S., 2019c. Dysconnectivity of multiple brain networks in schizophrenia: a meta-analysis of resting-state functional connectivity. Front. Psychiatry 10, 482. https://doi.org/10.3389/fpsyt.2019.00482.

Liao, J., Yan, H., Liu, Q., Yan, J., Zhang, L., Jiang, S., Zhang, X., Dong, Z., Yang, W., Cai, L., Guo, H., Wang, Y., Li, Z., Tian, L., Zhang, D., Wang, F., 2015. Reduced paralimbic system gray matter volume in schizophrenia: correlations with clinical variables, symptomatology and cognitive function. J. Psychiatr. Res. 65, 80–86. https://doi.org/10.1016/j.jpsychires.2015.04.008.

Liloia, D., Cauda, F., Nani, A., Manuello, J., Duca, S., Fox, P.T., Costa, T., 2018. Low entropy maps as patterns of the pathological alteration specificity of brain regions: a meta-analysis dataset. Data Brief 21, 1483–1495. https://doi.org/10.1016/j.dib.2018.10.142.

Liu, Y., Guo, W., Zhang, Y., Lv, L., Hu, F., Wu, R., Zhao, J., 2018. Decreased resting-state interhemispheric functional connectivity correlated with neurocognitive deficits in drug-naive first-episode adolescent-onset schizophrenia. Int. J. Neuropsychopharmacol. 21, 33–41. https://doi.org/10.1093/ijnp/pyx095.

Lorca-Puls, D.L., Gajardo-Vidal, A., White, J., Seghier, M.L., Leff, A.P., Green, D.W., Crinion, J.T., Ludersdorfer, P., Hope, T.M.H., Bowman, H., Price, C.J., 2018. The impact of sample size on the reproducibility of voxel-based lesion-deficit mappings. Neuropsychologia 115, 101–111. https://doi.org/10.1016/j.neuropsychologia.2018.03.014.

Lotze, M., Domin, M., Gerlach, F.H., Gaser, C., Lueders, E., Schmidt, C.O., Neumann, N., 2019. Novel findings from 2,838 adult brains on sex differences in gray matter brain volume. Sci. Rep. 9, 1671. https://doi.org/10.1038/s41598-018-38239-2.

Mallikarjun, P.K., Lalousis, P.A., Dunne, T.F., Heinze, K., Reniers, R.L., Broome, M.R., Farmah, B., Oyebode, F., Wood, S.J., Upthegrove, R., 2018. Aberrant salience network functional connectivity in auditory verbal hallucinations: a first episode psychosis sample. Transl. Psychiatry 8, 69. https://doi.org/10.1038/s41398-018-0118-6.

Mancuso, L., Costa, T., Nani, A., Manuello, J., Liloia, D., Gelmini, G., Panero, M., Duca, S., Cauda, F., 2019. The homotopic connectivity of the functional brain: a meta-analytic approach. Sci. Rep. 9, 3346. https://doi.org/10.1038/s41598-019-40188-3.

McDonald, C., Dineen, B., Hallahan, B., 2008. Meta-analysis of brain volumes in unaffected first-degree relatives of patients with schizophrenia overemphasizes hippocampal deficits. Arch. Gen. Psychiatry 65, 603–604. https://doi.org/10.1001/archpsyc.65.5.603 author reply 604-605.

McGorry, P.D., Hickie, I.B., Yung, A.R., Pantelis, C., Jackson, H.J., 2006. Clinical staging of psychiatric disorders: a heuristic framework for choosing earlier, safer and more effective interventions. Aust. N. Z. J. Psychiatry 40, 616–622. https://doi.org/10.1080/j.1440-1614.2006.01860.x.

Meisenzahl, E.M., Koutsouleris, N., Bottlender, R., Scheuerecker, J., Jager, M., Teipel, S. J., Holzinger, S., Frodl, T., Preuss, U., Schmitt, G., Burgermeister, B., Reiser, M., Born, C., Moller, H.J., 2008. Structural brain alterations at different stages of schizophrenia: a voxel-based morphometric study. Schizophr. Res. 104, 44–60. https://doi.org/10.1016/j.schres.2008.06.023.

Mendrek, A., Mancini-Marïe, A., 2016. Sex/gender differences in the brain and cognition in schizophrenia. Neurosci. Biobehav. Rev. 67, 57–78. https://doi.org/10.1016/j.neubiorev.2015.10.013.

Menon, V., Uddin, L.Q., 2010. Saliency, switching, attention and control: a network model of insula function. Brain Struct. Funct. 214, 655–667. https://doi.org/10.1007/s00429-010-0262-0.

Mier, D., Schirmbeck, F., Stoessel, G., Esslinger, C., Rausch, F., Englisch, S., Eisenacher, S., de Haan, L., Meyer-Lindenberg, A., Kirsch, P., Zink, M., 2019. Reduced activity and connectivity of left amygdala in patients with schizophrenia treated with clozapine or olanzapine. Eur. Arch. Psychiatry Clin. Neurosci. 269, 931–940. https://doi.org/10.1007/s00406-018-0965-4.

Mikolas, P., Melicher, T., Skoch, A., Matejka, M., Slovakova, A., Bakstein, E., Hajek, T., Spaniel, F., 2016. Connectivity of the anterior insula differentiates participants with first-episode schizophrenia spectrum disorders from controls: a machine-learning study. Psychol. Med. 46, 2695–2704. https://doi.org/10.1017/s0033291716000878.

Miller, T.J., McGlashan, T.H., Rosen, J.L., Cadenhead, K., Cannon, T., Ventura, J., McFarlane, W., Perkins, D.O., Pearlson, G.D., Woods, S.W., 2003. Prodromal assessment with the structured interview for prodromal syndromes and the scale of prodromal symptoms: predictive validity, interrater reliability, and training to reliability. Schizophr. Bull. 29, 703–715. https://doi.org/10.1093/oxfordjournals.schbul.a007040.

Mitelman, S.A., Nikiforova, Y.K., Canfield, E.L., Hazlett, E.A., Brickman, A.M., Shihabuddin, L., Buchsbaum, M.S., 2009. A longitudinal study of the corpus callosum in chronic schizophrenia. Schizophr. Res. 114, 144–153. https://doi.org/10.1016/j.schres.2009.07.021.

Moher, D., Liberati, A., Tetzlaff, J., Altman, D.G., 2009. Preferred reporting items for systematic reviews and meta-analyses: the PRISMA statement. J. Clin. Epidemiol. 62, 1006–1012. https://doi.org/10.1016/j.jclinepi.2009.06.005.

Mucci, A., Merlotti, E., Ucok, A., Aleman, A., Galderisi, S., 2017. Primary and persistent negative symptoms: concepts, assessments and neurobiological bases. Schizophr. Res. 186, 19–28. https://doi.org/10.1016/j.schres.2016.05.014.

Mukherjee, P., Whalley, H.C., McKirdy, J.W., Sprengelmeyer, R., Young, A.W., McIntosh, A.M., Lawrie, S.M., Hall, J., 2014. Altered amygdala connectivity within the social brain in schizophrenia. Schizophr. Bull. 40, 152–160. https://doi.org/10.1093/schbul/sbt086.

Müller, V.I., Cieslik, E.C., Serbanescu, I., Laird, A.R., Fox, P.T., Eickhoff, S.B., 2017. Altered brain activity in unipolar depression revisited: meta-analyses of neuroimaging studies. JAMA Psychiatry 74, 47–55. https://doi.org/10.1001/jamapsychiatry.2016.2783.

Müller, V.I., Cieslik, E.C., Laird, A.R., Fox, P.T., Radua, J., Mataix-Cols, D., Tench, C.R., Yarkoni, T., Nichols, T.E., Turkeltaub, P.E., Wager, T.D., Eickhoff, S.B., 2018. Ten simple rules for neuroimaging meta-analysis. Neurosci. Biobehav. Rev. 84, 151–161. https://doi.org/10.1016/j.neubiorev.2017.11.012.

Nakamura, K., Takahashi, T., Nemoto, K., Furuichi, A., Nishiyama, S., Nakamura, Y., Ikeda, E., Kido, M., Noguchi, K., Seto, H., Suzuki, M., 2013. Gray matter changes in subjects at high risk for developing psychosis and first-episode schizophrenia: a voxel-based structural MRI study. Front. Psychiatry 4, 16. https://doi.org/10.3389/fpsyt.2013.00016.

Nani, A., Manuello, J., Liloia, D., Duca, S., Costa, T., Cauda, F., 2019. The neural correlates of time: a meta-analysis of neuroimaging studies. J. Cogn. Neurosci. 1–31. https://doi.org/10.1162/jocn_a_01459.

Nenadic, I., Dietzek, M., Langbein, K., Sauer, H., Gaser, C., 2017. BrainAGE score indicates accelerated brain aging in schizophrenia, but not bipolar disorder. Psychiatry Res. Neuroimaging 266, 86–89. https://doi.org/10.1016/j.pscychresns.2017.05.006.

Nichols, T.E., Das, S., Eickhoff, S.B., Evans, A.C., Glatard, T., Hanke, M., Kriegeskorte, N., Milham, M.P., Poldrack, R.A., Poline, J.B., Proal, E., Thirion, B., Van Essen, D.C., White, T., Yeo, B.T., 2017. Best practices in data analysis and sharing in neuroimaging using MRI. Nat. Neurosci. 20, 299–303. https://doi.org/10.1038/nn.4500.

Nickl-Jockschat, T., Schneider, F., Pagel, A.D., Laird, A.R., Fox, P.T., Eickhoff, S.B., 2011. Progressive pathology is functionally linked to the domains of language and emotion: meta-analysis of brain structure changes in schizophrenia patients. Eur. Arch. Psychiatry Clin. Neurosci. 261 (Suppl 2), S166–171. https://doi.org/10.1007/s00406-011-0249-8.

Oertel, V., Knochel, C., Rotarska-Jagiela, A., Schonmeyer, R., Lindner, M., van de Ven, V., Haenschel, C., Uhlhaas, P., Maurer, K., Linden, D.E., 2010. Reduced laterality as a trait marker of schizophrenia–evidence from structural and functional neuroimaging. J. Neurosci. 30, 2289–2299. https://doi.org/10.1523/jneurosci.4575-09.2010.

Oertel-Knöchel, V., Linden, D.E., 2011. Cerebral asymmetry in schizophrenia. Neuroscientist 17, 456–467. https://doi.org/10.1177/1073858410386493.

Oertel-Knöchel, V., Knochel, C., Matura, S., Rotarska-Jagiela, A., Magerkurth, J., Prvulovic, D., Haenschel, C., Hampel, H., Linden, D.E., 2012. Cortical-basal ganglia imbalance in schizophrenia patients and unaffected first-degree relatives. Schizophr. Res. 138, 120–127. https://doi.org/10.1016/j.schres.2012.02.029.

Ortiz, B.B., Eden, F.D., de Souza, A.S., Teciano, C.A., de Lima, D.M., Noto, C., Higuchi, C. H., Cogo-Moreira, H., Bressan, R.A., Gadelha, A., 2017. New evidence in support of staging approaches in schizophrenia: differences in clinical profiles between first episode, early stage, and late stage. Compr. Psychiatry 73, 93–96. https://doi.org/10.1016/j.comppsych.2016.11.006.

Owen, M.J., Sawa, A., Mortensen, P.B., 2016. Schizophrenia. Lancet (London, England) 388, 86–97. https://doi.org/10.1016/s0140-6736(15)01121-6.

Palaniyappan, L., 2017. Progressive cortical reorganisation: a framework for investigating structural changes in schizophrenia. Neurosci. Biobehav. Rev. 79, 1–13. https://doi.org/10.1016/j.neubiorev.2017.04.028.

Palaniyappan, L., Liddle, P.F., 2012. Does the salience network play a cardinal role in psychosis? An emerging hypothesis of insular dysfunction. J. Psychiatry Neurosci. 37, 17–27. https://doi.org/10.1503/jpn.100176.

Pantelis, C., Yucel, M., Wood, S.J., Velakoulis, D., Sun, D., Berger, G., Stuart, G.W., Yung, A., Phillips, L., McGorry, P.D., 2005. Structural brain imaging evidence for multiple pathological processes at different stages of brain development in schizophrenia. Schizophr. Bull. 31, 672–696. https://doi.org/10.1093/schbul/sbi034.

Paracampo, R., Tidoni, E., Borgomaneri, S., di Pellegrino, G., Avenanti, A., 2017. Sensorimotor network crucial for inferring amusement from smiles. Cereb. Cortex (New York, N.Y. : 1991) 27, 5116–5129. https://doi.org/10.1093/cercor/bhw294.

Pergola, G., Selvaggi, P., Trizio, S., Bertolino, A., Blasi, G., 2015. The role of the thalamus in schizophrenia from a neuroimaging perspective. Neurosci. Biobehav. Rev. 54, 57–75. https://doi.org/10.1016/j.neubiorev.2015.01.013.

Radua, J., Mataix-Cols, D., 2012. Meta-analytic methods for neuroimaging data explained. Biol. Mood Anxiety Disord. 2, 6. https://doi.org/10.1186/2045-5380-2-6.

Radua, J., Mataix-Cols, D., Phillips, M.L., El-Hage, W., Kronhaus, D.M., Cardoner, N., Surguladze, S., 2012. A new meta-analytic method for neuroimaging studies that combines reported peak coordinates and statistical parametric maps. Eur. Psychiatry 27, 605–611. https://doi.org/10.1016/j.eurpsy.2011.04.001.

Radua, J., Rubia, K., Canales-Rodríguez, E.J., Pomarol-Clotet, E., Fusar-Poli, P., Mataix-Cols, D., 2014. Anisotropic kernels for coordinate-based meta-analyses of neuroimaging studies. Front. Psychiatry 5, 13. https://doi.org/10.3389/fpsyt.2014.00013.

Reid, M.A., White, D.M., Kraguljac, N.V., Lahti, A.C., 2016. A combined diffusion tensor imaging and magnetic resonance spectroscopy study of patients with schizophrenia. Schizophr. Res. 170, 341–350. https://doi.org/10.1016/j.schres.2015.12.003.

Ribolsi, M., Daskalakis, Z.J., Siracusano, A., Koch, G., 2014. Abnormal asymmetry of brain connectivity in schizophrenia. Front. Hum. Neurosci. 8, 1010. https://doi.org/10.3389/fnhum.2014.01010.

Rink, L., Pagel, T., Franklin, J., Baethge, C., 2016. Characteristics and heterogeneity of schizoaffective disorder compared with unipolar depression and schizophrenia - a systematic literature review and meta-analysis. J. Affect. Disord. 191, 8–14. https://doi.org/10.1016/j.jad.2015.10.045.

Saarinen, A.I.L., Huhtaniska, S., Pudas, J., Bjornholm, L., Jukuri, T., Tohka, J., Grano, N., Barnett, J.H., Kiviniemi, V., Veijola, J., Hintsanen, M., Lieslehto, J., 2020. Structural and functional alterations in the brain gray matter among first-degree relatives of schizophrenia patients: a multimodal meta-analysis of fMRI and VBM studies. Schizophr. Res. https://doi.org/10.1016/j.schres.2019.12.023.

Salomon, R., Progin, P., Griffa, A., Rognini, G., Do, K.Q., Conus, P., Marchesotti, S., Bernasconi, F., Hagmann, P., Serino, A., Blanke, O., 2020. Sensorimotor induction of auditory misattribution in early psychosis. Schizophr. Bull. https://doi.org/10.1093/schbul/sbz136.

Samartsidis, P., Montagna, S., Nichols, T.E., Johnson, T.D., 2017. The coordinate-based meta-analysis of neuroimaging data. Stat. Sci. 32, 580–599. https://doi.org/10.1214/17-STS624.

Samea, F., Soluki, S., Nejati, V., Zarei, M., Cortese, S., Eickhoff, S.B., Tahmasian, M., Eickhoff, C.R., 2019. Brain alterations in children/adolescents with ADHD revisited: a neuroimaging meta-analysis of 96 structural and functional studies. Neurosci. Biobehav. Rev. 100, 1–8. https://doi.org/10.1016/j.neubiorev.2019.02.011.

Scarpazza, C., De Simone, M.S., 2016. Voxel-based morphometry: current perspectives. Neurosci. Neuroecon. 5, 19–35. https://doi.org/10.2147/NAN.S66439.

Schiffer, B., Müller, B.W., Scherbaum, N., Forsting, M., Wiltfang, J., Leygraf, N., Gizewski, E.R., 2010. Impulsivity-related brain volume deficits in schizophrenia-

addiction comorbidity. Brain 133, 3093–3103. https://doi.org/10.1093/brain/awq153.
Seeley, W.W., Menon, V., Schatzberg, A.F., Keller, J., Glover, G.H., Kenna, H., Reiss, A.L., Greicius, M.D., 2007. Dissociable intrinsic connectivity networks for salience processing and executive control. J. Neurosci. 27, 2349–2356. https://doi.org/10.1523/JNEUROSCI.5587-06.2007.
Seidman, L.J., Mirsky, A.F., 2017. Evolving notions of schizophrenia as a developmental neurocognitive disorder. J. Int. Neuropsychol. Soc. 23, 881–892. https://doi.org/10.1017/s1355617717001114.
Shafiei, G., Markello, R.D., Makowski, C., Talpalaru, A., Kirschner, M., Devenyi, G.A., Guma, E., Hagmann, P., Cashman, N.R., Lepage, M., Chakravarty, M.M., Dagher, A., Misic, B., 2020. Spatial patterning of tissue volume loss in schizophrenia reflects brain network architecture. Biol. Psychiatry 87, 727–735. https://doi.org/10.1016/j.biopsych.2019.09.031.
Sheng, J., Zhu, Y., Lu, Z., Liu, N., Huang, N., Zhang, Z., Tan, L., Li, C., Yu, X., 2013. Altered volume and lateralization of language-related regions in first-episode schizophrenia. Schizophr. Res. 148, 168–174. https://doi.org/10.1016/j.schres.2013.05.021.
Shepherd, A.M., Laurens, K.R., Matheson, S.L., Carr, V.J., Green, M.J., 2012. Systematic meta-review and quality assessment of the structural brain alterations in schizophrenia. Neurosci. Biobehav. Rev. 36, 1342–1356. https://doi.org/10.1016/j.neubiorev.2011.12.015.
Shim, G., Oh, J.S., Jung, W.H., Jang, J.H., Choi, C.H., Kim, E., Park, H.Y., Choi, J.S., Jung, M.H., Kwon, J.S., 2010. Altered resting-state connectivity in subjects at ultra-high risk for psychosis: an fMRI study. Behav. Brain Funct. 6, 58. https://doi.org/10.1186/1744-9081-6-58.
Shimizu, M., Fujiwara, H., Hirao, K., Namiki, C., Fukuyama, H., Hayashi, T., Murai, T., 2008. Structural abnormalities of the adhesio interthalamica and mediodorsal nuclei of the thalamus in schizophrenia. Schizophr. Res. 101, 331–338. https://doi.org/10.1016/j.schres.2007.12.486.
Skåtun, K.C., Kaufmann, T., Brandt, C.L., Doan, N.T., Alnæs, D., Tønnesen, S., Biele, G., Vaskinn, A., Melle, I., Agartz, I., Andreassen, O.A., Westlye, L.T., 2018. Thalamo-cortical functional connectivity in schizophrenia and bipolar disorder. Brain Imaging Behav. 12, 640–652. https://doi.org/10.1007/s11682-017-9714-y.
Smieskova, R., Fusar-Poli, P., Allen, P., Bendfeldt, K., Stieglitz, R.D., Drewe, J., Radue, E. W., McGuire, P.K., Riecher-Rössler, A., Borgwardt, S.J., 2010. Neuroimaging predictors of transition to psychosis–a systematic review and meta-analysis. Neurosci. Biobehav. Rev. 34, 1207–1222. https://doi.org/10.1016/j.neubiorev.2010.01.016.
Smieskova, R., Marmy, J., Schmidt, A., Bendfeldt, K., Riecher-Rössler, A., Walter, M., Lang, U.E., Borgwardt, S., 2013. Do subjects at clinical high risk for psychosis differ from those with a genetic high risk?–A systematic review of structural and functional brain abnormalities. Curr. Med. Chem. 20, 467–481. https://doi.org/10.2174/0929867311320030018.
Spalletta, G., De Rossi, P., Piras, F., Iorio, M., Dacquino, C., Scanu, F., Girardi, P., Caltagirone, C., Kirkpatrick, B., Chiapponi, C., 2015. Brain white matter microstructure in deficit and non-deficit subtypes of schizophrenia. Psychiatry Res. 231, 252–261. https://doi.org/10.1016/j.pscychresns.2014.12.006.
Spreng, R.N., DuPre, E., Ji, J.L., Yang, G., Diehl, C., Murray, J.D., Pearlson, G.D., Anticevic, A., 2019. Structural covariance reveals alterations in control and salience network integrity in chronic schizophrenia. Cereb. Cortex (New York, N.Y. : 1991) 29, 5269–5284. https://doi.org/10.1093/cercor/bhz064.
Sugranyes, G., Kyriakopoulos, M., Dima, D., O'Muircheartaigh, J., Corrigall, R., Pendelbury, G., Hayes, D., Calhoun, V.D., Frangou, S., 2012. Multimodal analyses identify linked functional and white matter abnormalities within the working memory network in schizophrenia. Schizophr. Res. 138, 136–142. https://doi.org/10.1016/j.schres.2012.03.011.
Sun, Y., Chen, Y., Collinson, S.L., Bezerianos, A., Sim, K., 2015. Reduced hemispheric asymmetry of brain anatomical networks is linked to schizophrenia: a connectome study. Cereb. Cortex 27, 602–615. https://doi.org/10.1093/cercor/bhv255.
Tahmasian, M., Sepehry, A.A., Samea, F., Khodadadifar, T., Soltaninejad, Z., Javaheripour, N., Khazaie, H., Zarei, M., Eickhoff, S.B., Eickhoff, C.R., 2019. Practical recommendations to conduct a neuroimaging meta-analysis for neuropsychiatric disorders. Hum. Brain Mapp. https://doi.org/10.1002/hbm.24746.
Takahashi, T., Suzuki, M., 2018. Brain morphologic changes in early stages of psychosis: implications for clinical application and early intervention. Psychiatry Clin. Neurosci. 72, 556–571. https://doi.org/10.1111/pcn.12670.
Takayanagi, Y., Kulason, S., Sasabayashi, D., Takahashi, T., Katagiri, N., Sakuma, A., Obara, C., Nakamura, M., Kido, M., Furuichi, A., Nishikawa, Y., Noguchi, K., Matsumoto, K., Mizuno, M., Ratnanather, J.T., Suzuki, M., 2017. Reduced thickness of the anterior cingulate cortex in individuals with an at-risk mental state who later develop psychosis. Schizophr. Bull. 43, 907–913. https://doi.org/10.1093/schbul/sbw167.
Torres, U.S., Portela-Oliveira, E., Borgwardt, S., Busatto, G.F., 2013. Structural brain changes associated with antipsychotic treatment in schizophrenia as revealed by voxel-based morphometric MRI: an activation likelihood estimation meta-analysis. BMC Psychiatry 13, 342. https://doi.org/10.1186/1471-244x-13-342.
Torres, U.S., Duran, F.L., Schaufelberger, M.S., Crippa, J.A., Louza, M.R., Sallet, P.C., Kanegusuku, C.Y., Elkis, H., Gattaz, W.F., Bassitt, D.P., Zuardi, A.W., Hallak, J.E., Leite, C.C., Castro, C.C., Santos, A.C., Murray, R.M., Busatto, G.F., 2016. Patterns of regional gray matter loss at different stages of schizophrenia: a multisite, cross-sectional VBM study in first-episode and chronic illness. Neuroimage Clin. 12, 1–15. https://doi.org/10.1016/j.nicl.2016.06.002.
Turkeltaub, P.E., Eickhoff, S.B., Laird, A.R., Fox, M., Wiener, M., Fox, P., 2012. Minimizing within-experiment and within-group effects in Activation Likelihood Estimation meta-analyses. Hum. Brain Mapp. 33, 1–13. https://doi.org/10.1002/hbm.21186.
Uddin, L.Q., 2015. Salience processing and insular cortical function and dysfunction. Nat. Rev. Neurosci. 16, 55–61. https://doi.org/10.1038/nrn3857.
Vanasse, T.J., Fox, P.M., Barron, D.S., Robertson, M., Eickhoff, S.B., Lancaster, J.L., Fox, P.T., 2018. BrainMap VBM: an environment for structural meta-analysis. Hum. Brain Mapp. 39, 3308–3325. https://doi.org/10.1002/hbm.24078.
Velakoulis, D., Wood, S.J., McGorry, P.D., Pantelis, C., 2000. Evidence for progression of brain structural abnormalities in schizophrenia: beyond the neurodevelopmental model. Aust. N. Z. J. Psychiatry 34 (Suppl), S113–126. https://doi.org/10.1080/000486700231.
Velakoulis, D., Wood, S.J., Wong, M.T., McGorry, P.D., Yung, A., Phillips, L., Smith, D., Brewer, W., Proffitt, T., Desmond, P., Pantelis, C., 2006. Hippocampal and amygdala volumes according to psychosis stage and diagnosis: a magnetic resonance imaging study of chronic schizophrenia, first-episode psychosis, and ultra-high-risk individuals. Arch. Gen. Psychiatry 63, 139–149. https://doi.org/10.1001/archpsyc.63.2.139.
Vijayakumari, A.A., Thirunavukkarasu, P., Lukose, A., Arunachalam, V., Saini, J., Jain, S., Kutty, B.M., John, J.P., 2015. Exploration of the Effect of Demographic and Clinical Confounding Variables on Results of Voxel-Based Morphometric Analysis in Schizophrenia, Artificial Intelligence and Evolutionary Algorithms in Engineering Systems. Springer, pp. 139–149. https://doi.org/10.1007/978-81-322-2126-5_16.
Vita, A., De Peri, L., Deste, G., Barlati, S., Sacchetti, E., 2015. The effect of antipsychotic treatment on cortical gray matter changes in schizophrenia: does the class matter? A meta-analysis and meta-regression of longitudinal magnetic resonance imaging studies. Biol. Psychiatry 78, 403–412. https://doi.org/10.1016/j.biopsych.2015.02.008.
Vitolo, E., Tatu, M.K., Pignolo, C., Cauda, F., Costa, T., Ando, A., Zennaro, A., 2017. White matter and schizophrenia: a meta-analysis of voxel-based morphometry and diffusion tensor imaging studies. Psychiatry Res. Neuroimaging 270, 8–21. https://doi.org/10.1016/j.pscychresns.2017.09.014.
Voormolen, E.H., Wei, C., Chow, E.W., Bassett, A.S., Mikulis, D.J., Crawley, A.P., 2010. Voxel-based morphometry and automated lobar volumetry: the trade-off between spatial scale and statistical correction. NeuroImage 49, 587–596. https://doi.org/10.1016/j.neuroimage.2009.07.018.
Wang, C., Ji, F., Hong, Z., Poh, J.S., Krishnan, R., Lee, J., Rekhi, G., Keefe, R.S., Adcock, R.A., Wood, S.J., Fornito, A., Pasternak, O., Chee, M.W., Zhou, J., 2016. Disrupted salience network functional connectivity and white-matter microstructure in persons at risk for psychosis: findings from the LYRIKS study. Psychol. Med. 46, 2771–2783. https://doi.org/10.1017/s0033291716001410.
Wang, Q., Zhang, J., Liu, Z., Crow, T.J., Zhang, K., Palaniyappan, L., Li, M., Zhao, L., Li, X., Deng, W., Guo, W., Ma, X., Cheng, W., Ma, L., Wan, L., Lu, G., Liu, Z., Wang, J., Feng, J., Li, T., 2019. Brain Connectivity Deviates by Sex and Hemisphere in the First Episode of Schizophrenia"-A Route to the Genetic Basis of Language and Psychosis? Schizophr. Bull. 45, 484–494. https://doi.org/10.1093/schbul/sby061.
Watson, D.R., Anderson, J.M., Bai, F., Barrett, S.L., McGinnity, T.M., Mulholland, C.C., Rushe, T.M., Cooper, S.J., 2012. A voxel based morphometry study investigating brain structural changes in first episode psychosis. Behav. Brain Res. 227, 91–99. https://doi.org/10.1016/j.bbr.2011.10.034.
Winkler, A.M., Ridgway, G.R., Webster, M.A., Smith, S.M., Nichols, T.E., 2014. Permutation inference for the general linear model. NeuroImage 92, 381–397. https://doi.org/10.1016/j.neuroimage.2014.01.060.
Wojtalik, J.A., Smith, M.J., Keshavan, M.S., Eack, S.M., 2017. A systematic and meta-analytic review of neural correlates of functional outcome in schizophrenia. Schizophr. Bull. 43, 1329–1347. https://doi.org/10.1093/schbul/sbx008.
Wood, S.J., Yung, A.R., McGorry, P.D., Pantelis, C., 2011. Neuroimaging and treatment evidence for clinical staging in psychotic disorders: from the at-risk mental state to chronic schizophrenia. Biol. Psychiatry 70, 619–625. https://doi.org/10.1016/j.biopsych.2011.05.034.
Wright, I.C., McGuire, P.K., Poline, J.B., Travere, J.M., Murray, R.M., Frith, C.D., Frackowiak, R.S., Friston, K.J., 1995. A voxel-based method for the statistical analysis of gray and white matter density applied to schizophrenia. NeuroImage 2, 244–252. https://doi.org/10.1006/nimg.1995.1032.
Wright, I.C., Rabe-Hesketh, S., Woodruff, P.W., David, A.S., Murray, R.M., Bullmore, E. T., 2000. Meta-analysis of regional brain volumes in schizophrenia. Am. J. Psychiatry 157, 16–25. https://doi.org/10.1176/ajp.157.1.16.
Wylie, K.P., Tregellas, J.R., 2010. The role of the insula in schizophrenia. Schizophr. Res. 123, 93–104. https://doi.org/10.1016/j.schres.2010.08.027.
Yan, H., Tian, L., Yan, J., Sun, W., Liu, Q., Zhang, Y.B., Li, X.M., Zang, Y.F., Zhang, D., 2012. Functional and anatomical connectivity abnormalities in cognitive division of anterior cingulate cortex in schizophrenia. PLoS One 7, e45659. https://doi.org/10.1371/journal.pone.0045659.
Yung, A.R., Phillips, L.J., McGorry, P.D., McFarlane, C.A., Francey, S., Harrigan, S., Patton, G.C., Jackson, H.J., 1998. Prediction of psychosis. A step towards indicated prevention of schizophrenia. Br. J. Psychiatry 172, 14–20. https://doi.org/10.1192/S0007125000297602. Supplement.
Yung, A.R., Yuen, H.P., McGorry, P.D., Phillips, L.J., Kelly, D., Dell'Olio, M., Francey, S. M., Cosgrave, E.M., Killackey, E., Stanford, C., Godfrey, K., Buckby, J., 2005. Mapping the onset of psychosis: the comprehensive assessment of At-Risk mental

states. Aust. N. Z. J. Psychiatry 39, 964–971. https://doi.org/10.1080/j.1440-1614.2005.01714.x.

Zhang, Y., Zheng, J., Fan, X., Guo, X., Guo, W., Yang, G., Chen, H., Zhao, J., Lv, L., 2015. Dysfunctional resting-state connectivities of brain regions with structural deficits in drug-naive first-episode schizophrenia adolescents. Schizophr. Res. 168, 353–359. https://doi.org/10.1016/j.schres.2015.07.031.

Zhao, C., Zhu, J., Liu, X., Pu, C., Lai, Y., Chen, L., Yu, X., Hong, N., 2018. Structural and functional brain abnormalities in schizophrenia: a cross-sectional study at different stages of the disease. Prog. Neuropsychopharmacol. Biol. Psychiatry 83, 27–32. https://doi.org/10.1016/j.pnpbp.2017.12.017.